Science Translational Medicine
AAAS

# A human vaccine strategy based on chimpanzee adenoviral and MVA vectors that primes, boosts, and sustains functional HCV-specific T cell memory

Leo Swadling *et al.*

*Sci Transl Med* **6**, 261ra153 (2014);
DOI: 10.1126/scitranslmed.3009185

Editor's Summary

## An Ounce of HCV Prevention

Chronic hepatitis C virus (HCV) infection causes liver inflammation that can lead to diminished liver function or liver failure. Recent approval of antiviral drugs for HCV affords health care providers with treatment options; however, these new therapies are expensive with limited availability, leaving the door open for preventative approaches such as vaccines. Swadling *et al.* report a first-in-human trial of a prime-boost vaccine strategy for HCV. They prime with a simian adenoviral vector followed by a modified vaccinia Ankara vector encoding HCV proteins, which induces a T cell response similar to that found in HCV control in natural infection. If this strategy can show efficacy in later-stage studies, this approach could be used in a preventative HCV vaccine.



*Science Translational Medicine* (print ISSN 1946-6234; online ISSN 1946-6242) is published weekly, except the last week in December, by the American Association for the Advancement of Science, 1200 New York Avenue NW, Washington, DC 20005. 

HEPATITIS C VIRUS

# A human vaccine strategy based on chimpanzee adenoviral and MVA vectors that primes, boosts, and sustains functional HCV-specific T cell memory

Leo Swadling,[1]* Stefania Capone,[2]* Richard D. Antrobus,[1,3]* Anthony Brown,[1] Rachel Richardson,[1] Evan W. Newell,[4,5] John Halliday,[1,6] Christabel Kelly,[1,6] Dan Bowen,[1] Joannah Fergusson,[1] Ayako Kurioka,[1] Virginia Ammendola,[2] Mariarosaria Del Sorbo,[2] Fabiana Grazioli,[2] Maria Luisa Esposito,[2] Loredana Siani,[2] Cinzia Traboni,[2] Adrian Hill,[1,3] Stefano Colloca,[2] Mark Davis,[4] Alfredo Nicosia,[2,7,8] Riccardo Cortese,[9†] Antonella Folgori,[2] Paul Klenerman,[1,6] Eleanor Barnes[1,3,6‡]

**A protective vaccine against hepatitis C virus (HCV) remains an unmet clinical need. HCV infects millions of people worldwide and is a leading cause of liver cirrhosis and hepatocellular cancer. Animal challenge experiments, immunogenetics studies, and assessment of host immunity during acute infection highlight the critical role that effective T cell immunity plays in viral control. In this first-in-man study, we have induced antiviral immunity with functional characteristics analogous to those associated with viral control in natural infection, and improved upon a vaccine based on adenoviral vectors alone. We assessed a heterologous prime-boost vaccination strategy based on a replicative defective simian adenoviral vector (ChAd3) and modified vaccinia Ankara (MVA) vector encoding the NS3, NS4, NS5A, and NS5B proteins of HCV genotype 1b. Analysis used single-cell mass cytometry and human leukocyte antigen class I peptide tetramer technology in healthy human volunteers. We show that HCV-specific T cells induced by ChAd3 are optimally boosted with MVA, and generate very high levels of both $CD8^+$ and $CD4^+$ HCV-specific T cells targeting multiple HCV antigens. Sustained memory and effector T cell populations are generated, and T cell memory evolved over time with improvement of quality (proliferation and polyfunctionality) after heterologous MVA boost. We have developed an HCV vaccine strategy, with durable, broad, sustained, and balanced T cell responses, characteristic of those associated with viral control, paving the way for the first efficacy studies of a prophylactic HCV vaccine.**

## INTRODUCTION

Hepatitis C virus (HCV) infection is a leading cause of liver cirrhosis and hepatocellular cancer, with millions of people afflicted worldwide (*1*). Although new oral antivirals are available [reviewed in (*2*, *3*)], representing a real advance in the field, these are unaffordable and unavailable to most people, are least effective in patients with advanced liver disease, are associated with the development of viral resistance, and do not provide protection from reinfection (*4*). For these reasons, an effective vaccine to prevent chronic infection remains of clinical importance.

After primary infection, a proportion of those infected spontaneously resolve infection, leading to viral eradication and effectively representing long-term clinical cure (*1*, *5*). Therefore, an effective vaccine against HCV would not need to provide sterilizing immunity, but would aim to recapitulate or accelerate the immune pathway followed in natural infection to prevent disease chronicity.

HCV may be particularly susceptible to a T cell vaccination strategy (*6*). Although the correlates of protection in HCV are imperfectly defined, studies of host genetic and antiviral immune responses have shown that T cells play a critical role in viral control during primary infection. This is evidenced by associations of class I human leukocyte antigens [for example, HLA-A3, HLA-B27, and HLA-B57 (*7*–*9*)] and class II antigens [for example, HLA-DR1101 and HLA-DQ0301 (*10*)] with clearance, the temporal association of HCV-specific interferon-γ (IFN-γ)–secreting T cells with resolution of infection (*11*), and the generation of polyfunctional, durable $CD4^+$ and $CD8^+$ T cell subsets directed against multiple HCV antigens in spontaneous control (*5*, *12*). Additionally, the depletion of $CD4^+$ and $CD8^+$ T cell subsets in chimpanzees is associated with viral persistence after challenge (*13*, *14*), whereas secondary exposure to HCV in intravenous drug users (IVDUs) is associated with the generation of robust T cell immunity (*15*), which correlates with protection from chronic infection upon subsequent exposure to HCV. Together, these data suggest that an HCV T cell vaccine could prevent persistent HCV infection.

Although broadly neutralizing antibodies have been identified (*16*) and may contribute to viral control both in natural infection (*15*, *17*) and in chimpanzee challenge models after vaccination with HCV envelope proteins (*18*), it is not yet possible to generate these in most people by vaccination (*19*). In contrast, the development of a potent T cell vaccine is a practical and attainable goal. Proof of principle that a prophylactic T cell vaccine for HCV may be an effective strategy was first obtained in a chimpanzee model. High

[1]Nuffield Department of Medicine, University of Oxford, Oxford OX1 3SY, UK. [2]ReiThera Srl (ex Okairos), Viale Città d'Europa 679, 00144 Rome, Italy. [3]The Jenner Institute, University of Oxford, Oxford OX3 7DQ, UK. [4]Department of Microbiology and Immunology, Stanford University, Stanford, CA 94305, USA. [5]Singapore Immunology Network, Singapore 138648, Singapore. [6]National Institute for Health Research Oxford Biomedical Research Centre, and Translational Gastroenterology Unit, Oxford OX3 7LE, UK. [7]CEINGE, via Gaetano Salvatore 486, 80145 Naples, Italy. [8]Department of Molecular Medicine and Medical Biotechnology, University of Naples Federico II, Via S. Pansini 5, 80131 Naples, Italy. [9]Okairos AG, 4051 Basel, Switzerland.
*These authors contributed equally to this work.
†Present address: Keires AG, Elisabethenstrasse 15, 4051 Basel, Switzerland.
‡Corresponding author. E-mail: ellie.barnes@ndm.ox.ac.uk

levels of anti-HCV–specific T cell immunity were induced in animals vaccinated with adenoviral (Ad) and DNA vectors encoding the nonstructural (NS) HCV proteins (*20*); after heterologous viral challenge, four of five vaccinated animals developed low-level viremia and minimal hepatitis, followed by accelerated viral clearance.

To overcome the issue of preexisting anti-Ad immunity in humans, which may limit vaccine efficacy (*21*), we developed a large panel of replication-defective chimpanzee and human adenoviruses found at low seroprevalence that could be used as vaccine vectors (*22*, *23*). We trialed the first HCV prophylactic T cell vaccine using heterologous Ad vectors derived from human (Ad6) and chimpanzees (ChAd3) encoding the HCV NS3-NS5B polyprotein, with a genetically inactivated NS5B polymerase (*24*) in healthy volunteers. The magnitude and breadth of polyfunctional HCV-specific T cells induced after a single priming vaccination with either vector were the most potent described to date in human studies (*25*). However, there were two limitations: first, heterologous Ad boosting failed to increase T cell responses to the level observed after priming. Subsequent analysis showed that this was most likely due to the induction of cross-reactive anti-Ad antibodies. This was unexpected because heterologous Ad vaccination using the same vectors in macaques had generated substantial responses after boosting, suggesting that the vectors were serologically distinct. Second, $CD8^+$ T cells were the dominant subset induced by vaccination, whereas natural history, genetic, and T cell depletion studies show that both $CD4^+$ and $CD8^+$ T cell subsets are critical for viral control (*5*, *11*–*15*, *26*–*29*).

Here, we have overcome these limitations and developed an HCV prophylactic T cell vaccination strategy based on heterologous viral vectors [ChAd3 and modified vaccinia Ankara (MVA)] that is highly immunogenic after both priming and boosting vaccination, inducing both $CD4^+$ and $CD8^+$ T cells targeting multiple HCV antigenic targets, and associated with an acceptable safety profile.

We elected to use ChAd3 rather than Ad6 because the seroprevalence of ChAd3 is markedly lower than Ad6 (3% versus 28%), and in a heterologous Ad vectored vaccine regime, boosting after ChAd3 prime was optimal (*25*). Additionally, we have performed a comprehensive characterization of vaccine-induced T cell phenotype and functionality using both traditional cytometry and (for the first time in a clinical trial) cytometry by time of flight (CyTOF), revealing that this vaccine induced a functional T cell memory profile.

## RESULTS

### Vaccination with ChAd3-NSmut and MVA-NSmut is well tolerated

Vaccines were administered intramuscularly, and the volunteer group protocols are described in table S1. Most local and systemic adverse events (AEs) were mild or moderate (92%) and resolved within 48 hours. Systemic AEs were more common after MVA-NSmut (mean number/volunteer; 4.1 MVA-NSmut versus 1.9 ChAd3-NSmut; $P = 0.032$). The proportion of volunteers experiencing one or more moderate/severe AE was not significantly different between the two vaccines ($P = 0.689$). Severe AEs were observed in five volunteers after MVA-NSmut and two volunteers after ChAd3-NSmut (local pain/swelling, fatigue, migraine, and feverishness), but these resolved within 24 to 48 hours. Overall, both ChAd3-NSmut and MVA-NSmut were very well tolerated with no serious adverse reactions (fig. S1).

### MVA-NSmut optimally and specifically boosts HCV-specific T cell responses after ChAd3-NSmut priming without the induction of regulatory T cells

We previously showed that boosting with heterologous Ad6-NSmut did not enhance anti-HCV immune responses above magnitudes observed with ChAd3-NSmut prime vaccination (*25*). We therefore evaluated the immunogenicity of a heterologous MVA-NSmut boost [$2 \times 10^8$ plaque-forming units (pfu)] 8 weeks after ChAd3-NSmut [$2.5 \times 10^{10}$ viral particles (vp)] prime in nine healthy volunteers (arm A2, table S1) using IFN-γ enzyme-linked immunospot (ELISpot). All volunteers responded to ChAd3-NSmut prime, peaking 2 to 4 weeks after vaccination [median, 1140; range, 87 to 4427 spot-forming cells (SFCs)/$10^6$ peripheral blood mononuclear cells (PBMCs); Fig. 1A]. HCV-specific T cell responses were significantly enhanced by MVA-NSmut boost in all volunteers, peaking 1 week after vaccination (median, 2355; range, 1490 to 6117 SFCs/$10^6$ PBMCs; peak after ChAd3-NSmut prime versus peak after MVA-NSmut boost; $P = 0.0039$; Fig. 1, A and B). Furthermore, in comparison to heterologous Ad vaccination, ChAd3-NSmut/MVA-NSmut prime-boost generated responses that were more sustained over time, and significantly greater at the end of the study both to the HCV NS region overall (Fig. 1, B and C; median, 443; range, 138 to 1783 versus median, 98; range, 10 to 1092 SFCs/$10^6$ PBMCs; $P = 0.0109$) and to all six individual peptide pools covering HCV NS (Fig. 1D). The peak response after MVA-NSmut boost correlated significantly with the durability of the T cell response [trial week 9 (TW9) versus TW34; linear regression $R^2 = 0.784$; $P = 0.0034$; Fig. 1E) and between TW8 (before MVA-NS boost vaccination; $R^2 = 0.68$; $P = 0.0429$). T cell responses remained detectable by IFN-γ ELISpot in four of five patients tested at weeks 70 to 73 (median, 302; range, 10 to 732 SFCs/$10^6$ PBMCs; Fig. 1A).

No HCV-specific T cell response was detected in the four volunteers vaccinated with $2 \times 10^8$ pfu MVA-NSmut prime alone (arm A1; table S3).

To assess a possible nonspecific "bystander" expansion of non-HCV antigen-specific T cells after vaccination, we monitored the T cell response to HLA class I influenza A (FLU), Epstein-Barr virus (EBV), and cytomegalovirus (CMV) epitopes and to CMV lysate; no change in the magnitude of the responses to these antigens was observed (fig. S2). The induction of regulatory T cells ($T_{regs}$) was also assessed in five volunteers before vaccination, at the peak of the T cell response to ChAd3-NSmut prime and MVA-NS boost vaccination (TW2–4 and TW9, respectively), and long-term (TW47–72) after vaccination. We found no significant change in the magnitude of $T_{reg}$ subsets, and levels of $T_{regs}$ in vaccinated volunteers were comparable to those seen in PBMCs from eight healthy unvaccinated volunteers (fig. S3).

### MVA-NSmut boost increases the breadth of ChAd3-NSmut–primed T cell responses

We compared the breadth of T cell responses induced by ChAd3-NSmut prime/MVA-NSmut boost to that induced by heterologous Ad boosting using peptides corresponding to the entire immunogen in six pools and defined further using 8 to 11 peptides in minipools (Table 1). At the peak response after MVA-NSmut boost, most individuals responded to all six peptide pools (range, 4 to 6; Fig. 2, A and B), and the breadth was significantly higher than that observed after ChAd3-NSmut prime or after heterologous Ad boost (Fig. 2, A and C; $P = 0.0156$ and $P = 0.0010$, respectively). The breadth of response was also significantly greater at the end of the study after MVA vaccination

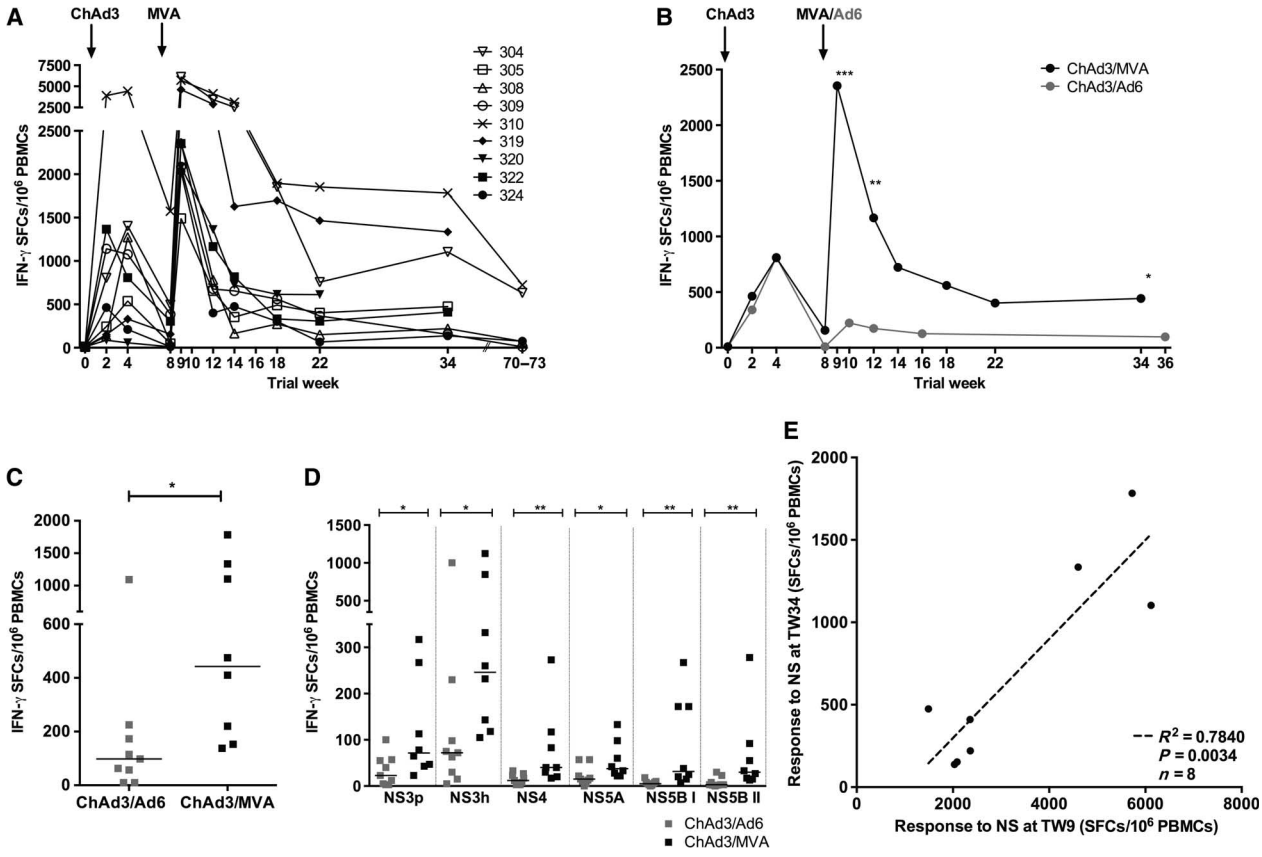


**Fig. 1. Magnitude of T cell responses to HCV NS after vaccination.** (**A** to **D**) The total ex vivo IFN-γ ELISpot response to the NS region of HCV is shown over time during the vaccine trial (calculated by summing the responses to positive peptide pools corrected for background; see Materials and Methods). (A) The kinetics of the response is shown for the nine volunteers who received ChAd3-NSmut/MVA-NSmut vaccination. Four volunteers were assessed at an extra time point a year and half after initial vaccination (TW70–73). (B) The median ex vivo IFN-γ ELISpot response to HCV NS is shown for volunteers receiving ChAd3-NSmut/MVA-NSmut (black; $n = 9$) or ChAd3-NSmut/Ad6-NSmut (gray; $n = 9$) vaccine regimens. Arrows indicate vaccinations, and trial week indicates weeks since prime vaccination (ChAd3/MVA TW12 versus ChAd3/Ad6 TW12, $P = 0.0012$; ChAd3/MVA TW9 versus ChAd3/Ad6 TW10, $P = 0.0009$). (C and D) A comparison of the total ex vivo response to HCV NS at TW34–36 in volunteers receiving ChAd3-NSmut/MVA-NSmut (black) or ChAd3-NSmut/Ad6-NSmut (gray) vaccinations ($P = 0.0109$) by IFN-γ ELISpot. (C) Magnitude of summed total T cell response to HCV NS. (D) Magnitude of T cell response to six peptide pools covering HCV NS. (**E**) Magnitude of response to HCV NS at the peak after MVA-NSmut vaccination (TW9) versus the end of the study (TW34) for volunteers receiving ChAd3-NSmut/MVA-NSmut vaccinations with linear regression (no TW34 data available for volunteer 320).

when compared to heterologous Ad boost vaccination ($P = 0.0355$; Fig. 2A). Further dissection of responses to minipool level revealed that the number of HCV epitopes targeted after MVA boost was as high as 31 in a single individual (subject 310; Table 1); because the minipool analysis was performed at TW12, after contraction of the T cell response, the true number of epitopes targeted in each subject may be underestimated. Although all peptide pools were targeted in patients from diverse HLA backgrounds, responses to NS3 dominated after both ChAd3 prime and MVA boost [Friedman analysis of variance (ANOVA), $P = 0.0033$; Fig. 2, B and C]. MVA boost increased the magnitude but did not affect the overall hierarchy of HCV antigen recognition (Fig. 2C). Responses to two epitopes located in NS3h restricted by HLA-A1 and HLA-A2 (marked bold in Table 1) were particularly prevalent and selected for subsequent pentamer analysis.

All individuals showed a major increase in T cell response with MVA boost compared to Ad prime, but three individuals showed a particularly strong response to MVA boost vaccination (Fig. 1A); however, there were no known differences in the three "super-responders" when compared to the other volunteers: In particular, no one HLA type was overrepresented in these three volunteers, and there was no evidence that these volunteers had previous exposure to HCV. After removing the super-responders from the analysis, the difference between Ad6-NSmut and MVA-NSmut boost vaccination remained statistically significant at multiple time points, including the end of the study TW34/36 ($P = 0.0287$).

## T cell responses after MVA-NSmut boosting vaccination recognize multiple HCV genotypes

We determined the capacity of the T cells induced by ChAd3-NSmut/MVA-NSmut encoding the genotype 1b immunogen to target other globally prevalent HCV subtypes using peptides derived from genotypes 1a, 3a, and 4a sequences in IFN-γ ELISpot assays. Although subtypes 1a, 3a, and 4a diverge significantly from genotype 1b at the amino acid level (86, 77, and 78% sequence homology, respectively),

**Table 1. Specificity of T cell response to HCV NS after vaccination.** The peptide pools that were positive [see Materials and Methods; >48 SFCs/$10^6$ PBMCs and 3× dimethyl sulfoxide (DMSO) by ELISpot assay] at the peak of the T cell response after ChAd3-NSmut/MVA-NSmut vaccination (TW9) are shown with each volunteer's HLA type. Where possible, T cell responses were further mapped to minipool (at TW12), 15-mer peptide, or optimal peptide. The immunodominant responses to peptides 103 and 95 (pool G; NS3) in HLA-A1 and HLA-A2 donors, respectively, are shown in bold and were tracked using major histocompatibility complex (MHC) class I multimers.

| Volunteer | HLA | A | HLA | B | HLA | C | Positive pools | Minipools | Peptide (minipool:peptide number-seqence) | Optimal (HLA restriction) |
|---|---|---|---|---|---|---|---|---|---|---|
| 304 | 11 | | 39 | 57 | 12 | 6 | F | Fb, Fd, Ff, Fh | Fb:11-QSFLATCVNGVCWTV/12-ATCVNGVCWTVYHGA | Fb: CVNGVCWTV (A2) |
| | | | | | | | G | Ge, Gf, Gg, Gh | Gh:153-VTLTHPITKYIMACM | Gh: TLTHPITK (A11) |
| | | | | | | | H | Ha, Hd, Hf | Ha:164-SVVIVGRIILSGRPA; Hf:207-ILAGYGAGVAGALVA | |
| | | | | | | | I | Ib, Ic, Id, Ii | | |
| | | | | | | | L | Lc, Lf | Lf:400-LVNTWKSKKNPMGFS/401-WKSKKNPMGFSYDTR | Lf: KSKKNPMG (B57) |
| | | | | | | | M | Mc, Md, Mf | Mc: 444-RVYYLTRDPTTPLAR/445-LTRDPTTPLARAAWE | Mc: LTRDPTTPLAR |
| 305 | 11 | **1** | 44 | 52 | 5 | 12 | F | Fe, Ff, Fh | Ff: 56-QGYKVLVLNPSVAAT/57-VLVLNPSVAATLGFG | Ff: VLVLNPSVAAT |
| | | | | | | | **G** | **Gc**, Ge,Gg, Gh | **Gc: 103-VATDALMTGYTGDFD**; Gh: 149-HGPTPLLYRLGAVQN/150-PLLYRLGAVQNEVTL | **Gc: ATDALMTGY (A1);** Gh: PLLYRLGAVQN |
| | | | | | | | H | Ha, Hd | | |
| | | | | | | | I | Ii | | |
| | | | | | | | M | Mf | | |
| 308 | **2** | **1** | 8 | 44 | 5 | 7 | F | Fb | Fb:11-QSFLATCVNGVCWTV/12-ATCVNGVCWTVYHGA | Fb: CVNGVCWTV (A2) |
| | | | | | | | **G** | **Gb, Gc** | **Gb: 95-LAAKLSGLGINAVAY; Gc: 103-VATDALMTGYTGDFD** | **Gb: KLSGLGINAV (A2); Gc: ATDALMTGY (A1)** |
| | | | | | | | H | | | |
| | | | | | | | I | Ih | | |
| | | | | | | | L | | | |
| | | | | | | | M | Mf | | |
| 309 | 11 | | 35 | | 4 | | F | Fg | | |
| | | | | | | | G | Ga, Gg, Gh | Ga: 83-VTVPHPNIEEVALSN/84-HPNIEEVALSNTGEI; Gh: 153-VTLTHPITKYIMACM | Ga: HPNIEEVAL (B35); Gh: TLTHPITKY (A11) |
| | | | | | | | H | Hd | | |
| | | | | | | | I | | | |
| | | | | | | | M | | | |
| 310 | 3 | **2** | 35 | 65 | 4 | 8 | F | Fa, Fb, Fc, Fd, Ff, Fh | Fb:11-QSFLATCVNGVCWTV/12-ATCVNGVCWTVYHGA | Fb: CVNGVCWTV (A2) |
| | | | | | | | **G** | Ga, **Gb**, Gc, Gd, Ge, Gf, Gg, Gh, | Ga: 83-VTVPHPNIEEVALSN/84-HPNIEEVALSNTGEI; **Gb: 95-LAAKLSGLGINAVAY** | **Gb: KLSGLGINAV (A2)** |
| | | | | | | | H | Ha, Hb, Hd, He, Hf, Hg, Hh | Hf:207-ILAGYGAGVAGALVA | |
| | | | | | | | I | Ib, Ic, Id, Ie, If, Ig, Ij, | | |
| | | | | | | | L | Lc, Le | Le:391-RVCEKMALYDVVSTL | |
| | | | | | | | M | Mg | | |

continued on next page

| Volunteer | HLA A | HLA B | HLA C | Positive pools | Minipools | Peptide (minipool:peptide number-seqence) | Optimal (HLA restriction) |
|---|---|---|---|---|---|---|---|
| 319 | **2** 13 | 57 | 6 | F | Fa, Fb, Fd | Fa:10-STATQSFLATCVNGV; Fb:11-QSFLATCVNGVCWTV/12-ATCVNGVCWTVYHGA | Fb: CVNGVCWTV (A2) |
| | | | | **G** | **Gb**, Gc, Ge, Gf | **Gb: 95-LAAKLSGLGINAVAY;** Gf: 129-LRAYLNTPGLPVCQD | Ga: HPNIEEVAL (B35); **Gb: KLSGLGINAV (A2)** |
| | | | | H | Hf | Hf:207-ILAGYGAGVAGALVA | |
| | | | | I | Ic, Id | Ic: 264-SRALWRVAAEEYVEV; Id: 274-PEFFTEVDGVRLHRY | |
| | | | | L | Lc, Lf | Lf:400-LVNTWKSKKNPMGFS/401-WKSKKNPMGFSYDTR | Lf: KSKKNPMG (B57) |
| 320 | 3 **1** 7 | | 7 | **G** | Gb, **Gc**, Gd | Gb: 97-GINAVAYYRGLDVSV; **Gc: 103-VATDALMTGYTGDFD**; Gd: 118-RRGIYRFVTPGERPS | **Gc: ATDALMTGY (A1)** |
| | | | | H | | | |
| | | | | I | Ic | | |
| | | | | L | | | |
| | | | | M | | | |
| 322 | **2** 31 | 27 7 | 7 2 | F | Fb | Fb:11-QSFLATCVNGVCWTV/12-ATCVNGVCWTVYHGA | Fb: CVNGVCWTV (A2) |
| | | | | **G** | **Gb** | **Gb: 95-LAAKLSGLGINAVAY** | **Gb: KLSGLGINAV (A2)** |
| | | | | H | Hh | | |
| | | | | M | Md, Mg | Md: 454-WARMILMTHFFSILL; Mg: 489-IYHSLSRARPRWFML/490-LSRARPRWFMLCLLL | |
| 324 | **1** 8 | | 7 | F | | | |
| | | | | **G** | **Gc**, Gd, Gh | **Gc: 103-VATDALMTGYTGDFD**; Gd: 109-TQTVDFSLDPTFTIE/110-DFSLDPTFTIETTTV; Gh: 153-VTLTHPITKYIMACM | **Gc: ATDALMTGY (A1);** Gh: TLTHPITKY (A11) |
| | | | | H | Hb | Hb: 167-RPAIVPDREFLYQEF | |
| | | | | I | | | |
| | | | | L | Le | Le:388-PARLIVFPDLGVRVC | |
| | | | | M | | | |

responses to these subtypes were generated, albeit at a lower magnitude (Fig. 2D). Responses to genotype 1a were about 60%, and to genotype 3a/4a were 30% of those generated against genotype 1b, whereas breadth is maintained (fig. S4). We observed a direct correlation between the response to the genotype 1b immunogen and subtypes 1a and 3a but not to 4a (1b versus 1a: $R^2 = 0.974$, $P = 0.0018$; 1b versus 3a: $R^2 = 0.975$, $P = 0.0017$; 1b versus 4a: $R^2 = 0.045$, $P = 0.734$).

### MVA-NSmut boost induces polyfunctional CD4 and CD8$^+$ T cell subsets

Next, we assessed the relative contribution and functionality of CD4$^+$ and CD8$^+$ T cell subsets to the total response. We found that MVA-NSmut boosting vaccination induced higher numbers of both T cell subsets compared to those seen after ChAd3-NSmut prime, and also in comparison to heterologous Ad6-NSmut boost (Fig. 3). Using intracellular cytokine staining (ICS) and SPICE analysis, we showed that vaccine-induced HCV-specific CD4$^+$ and CD8$^+$ T cells were polyfunctional with an equal proportion of CD4$^+$ T cells producing one [interleukin-2 (IL-2) or IFN-γ], two [IL-2 and IFN-γ or IFN-γ and tumor necrosis factor–α (TNFα)], or three (IL-2, IFN-γ, and TNFα) cytokines, whereas CD8$^+$ T cells predominantly produced IFN-γ early after vaccination (TW4/TW9) and produced IFN-γ in conjunction with TNFα or TNFα and IL-2 10 to 14 weeks after boost (fig. S5). The polyfunctionality of CD4$^+$ and CD8$^+$ T cells increased after MVA vaccination, peaking at weeks 18 and 22, respectively (fig. S5). We also assessed the per-cell production of cytokine in polyfunctional compared to single cytokine-producing T cells (fig. S6). The geometric mean fluorescent intensity (GeoMFI) of each cytokine (with the exception of IL-2 production by CD8$^+$ cells) was significantly higher in CD4$^+$ and CD8$^+$ T cells that produced three cytokines versus one cytokine. The biggest differences were seen in per-cell production of IFN-γ [median GeoMFI of triple- versus single-producing CD4$^+$ T cells was 4131 versus 1322 ($P < 0.0001$), and 10,329 versus 1543 for CD8$^+$ T cells ($P < 0.0001$)]. Polyfunctional CD4$^+$ and CD8$^+$ T cells were readily detectable by ICS 74 weeks after prime vaccination (Fig. 3B).

The proliferative capacity of PBMCs was assessed in [$^3$H]thymidine incorporation assays. HCV recombinant protein antigens were used in

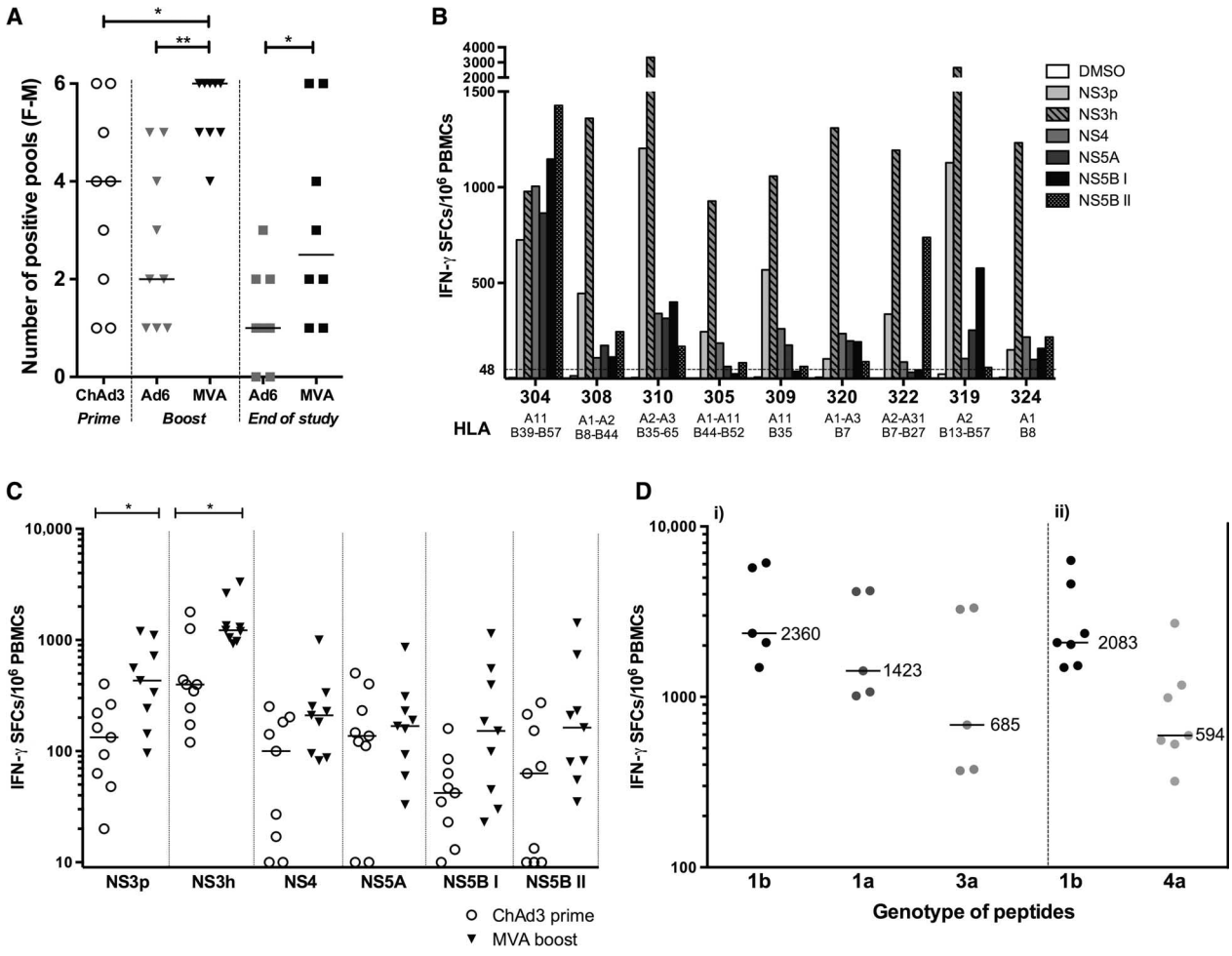


**Fig. 2. Breadth, specificity, and cross-reactivity of T cell responses to HCV NS after vaccination.** (**A**) Breadth of the T cell response to HCV NS [the number of positive pools (F-M)] assessed ex vivo at peak magnitude after ChAd3-NSmut prime vaccination (TW2–4; open circles), after MVA-NSmut boost (TW9; black triangles) or Ad6-NSmut boost (TW12–16; gray triangles), and at the end of the study (EOS; TW34–36) after MVA-NSmut boost (black squares) or Ad6-NSmut boost (gray squares) measured by IFN-γ ELISpot. Bars, median (ChAd3 prime versus MVA boost, $P = 0.0156$; Ad6 boost versus MVA boost, $P = 0.0010$; Ad6 EOS versus MVA EOS, $P = 0.0355$). (**B**) The magnitude of the T cell response to individual peptide pools 1 week after boost (TW9) is shown for volunteers who received ChAd3-NSmut/MVA-NSmut vaccination (IFN-γ ELISpot). (**C**) The peak magnitude of the T cell response to each individual pool is shown for volunteers vaccinated with ChAd3-NSmut/MVA-NSmut ($n = 9$) after ChAd3-NSmut prime vaccination (TW2–4; open circles) and after MVA-NSmut boost vaccination (TW9; black triangles; IFN-γ ELISpot; ChAd3/Ad6 versus ChAd3/MVA pool F: $P = 0.0106$, pool G: $P = 0.0106$). (**D**) Cross-reactivity of T cell response: total magnitude of T cell responses using peptide pools covering the NS region of HCV genotype 1b (vaccine strain) compared to (i) genotypes 1a and 3a and (ii) genotype 4a in volunteers by IFN-γ ELISpot assay at TW9. Bars at median with values shown (SFCs/$10^6$ PBMCs).

this assay, which detects predominantly $CD4^+$ T cell proliferation. Strong proliferative responses to multiple HCV antigens could be detected 6 weeks after MVA-NSmut boost, and these increased further when assessed 26 weeks after MVA-NSmut boost (Wilcoxon, $P = 0.0391$, NS3; Fig. 3D), consistent with the generation of a population of memory T cells capable of rapid proliferation on reexposure to antigen. Proliferative responses after MVA-NSmut boost were significantly greater than those seen after heterologous Ad boost (Fig. 3D).

### A detailed characterization of vaccine-induced $CD8^+$ T cells was performed using HLA class I multimers

After fine mapping of vaccine-induced T cell responses (Table 1), we used HLA class I pentamers (HLA-A*0201 HCV $NS3_{1406–1415}$ KLSALGINAV; HLA-A*0101 HCV $NS3_{1435–1443}$ ATDALMTGY) to track the characteristics of vaccine-induced T cells over time (Fig. 4, A and B; example FACS plots in fig. S7). After boosting with MVA-NSmut, HCV-specific T cells were highly activated, expressing CD38 in 80 to 100% $pentamer^+$ cells, with about 60% coexpressing HLA-DR (Fig. 4C). In contrast, after heterologous Ad boosting, 25% expressed CD38 with minimal HLA-DR coexpression. PD-1 expression (a molecule that has been associated with both T cell activation and exhaustion) was also high after MVA-NSmut, declining over the duration of the study (Fig. 4C). HCV-specific T cells after MVA-NSmut also expressed granzyme A, granzyme B, and variable levels of perforin (Fig. 4D).

After ChAd3-NSmut priming vaccination, a mixed pool of memory populations was detected [central memory T cells ($T_{cm}$; $CD45RA^-CCR7^+$),

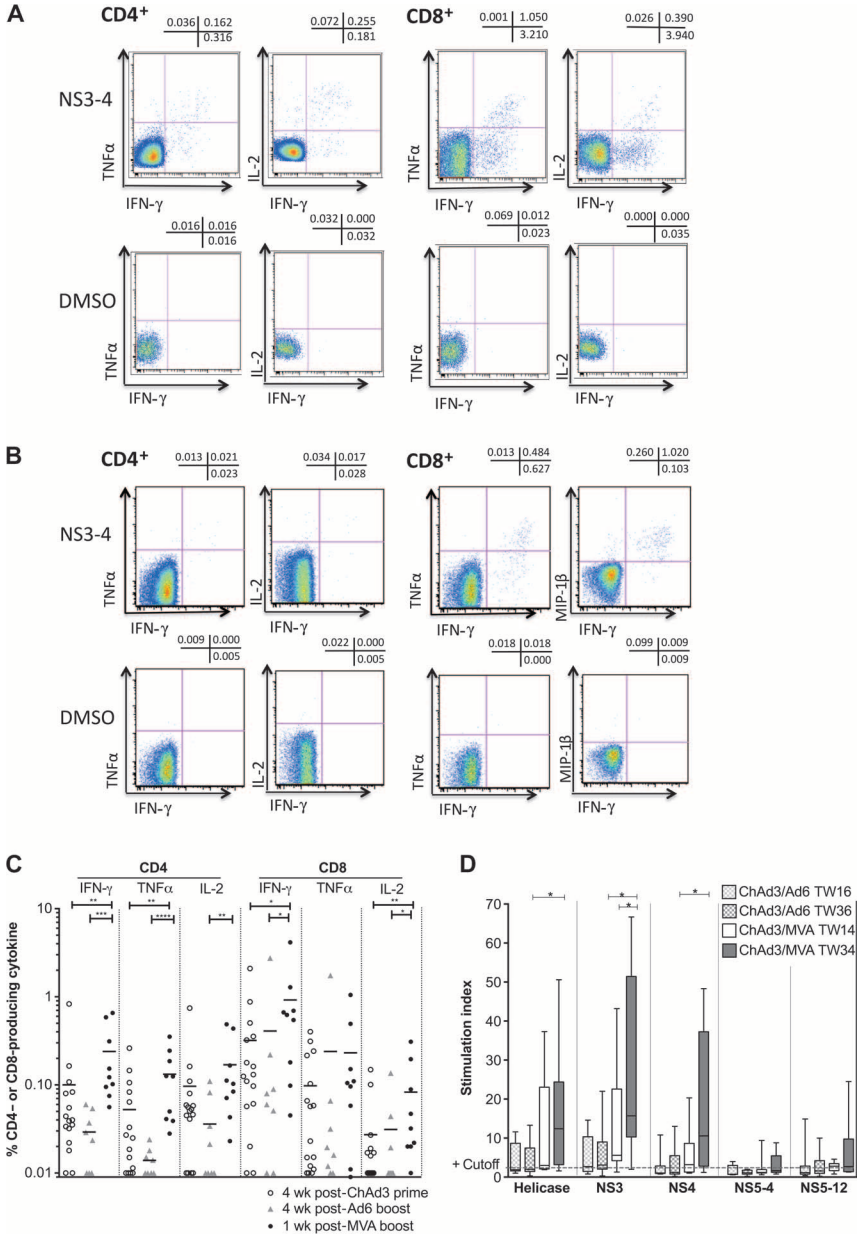


**Fig. 3. Functionality of vaccine-induced CD4$^+$ and CD8$^+$ T cells.** (**A** and **B**) Example fluorescence-activated cell sorting (FACS) plots showing TNFα/IFN-γ and IL-2/IFN-γ after ICS are shown for CD4$^+$ and CD8$^+$ T cells stimulated with NS3–4 or DMSO control in volunteer 310 (A) 1 week and (B) 62 weeks after MVA-NSmut boost vaccination (TW9 and TW70, respectively). (**C**) Comparison of cytokine production by T cells at peak response after vaccination. The percentage of total CD4$^+$ or CD8$^+$ T cells producing IFN-γ, TNFα, or IL-2 after stimulation with NS3–5 is shown at the peak after ChAd3-NSmut prime vaccination (open circles; TW4, $n$ = 16) and at the peak after boost vaccination with either heterologous Ad6-NSmut (gray triangles; TW12, $n$ = 8) or MVA-NSmut (filled circles; TW9, $n$ = 9). PBMCs were stimulated with pools F + G + H (NS3–4) or I + L + M (NS5) overnight, and the percentage of cytokine-secreting cells for these two stimulations were summed after background subtraction (DMSO stimulation) to get the total NS response. Values ≤0.01 are assigned 0.01. Bars, median. (**D**) Proliferative capacity of T cells after boost vaccination: proliferative response to stimulation with HCV proteins, plotted as box and whisker plots (max-min, interquartile range, and median), is shown 6 to 8 weeks (TW14/16) and 26 to 28 weeks (TW34/36) after boost vaccination for ChAd3-NSmut/Ad6-NSmut (checkered bars; $n$ = 9) and ChAd3-NSmut/MVA-NSmut (solid bars; $n$ = 9) groups. Data are expressed as stimulation index (SI). A dashed line at SI = 3 indicates positivity cutoff (data shown in table S4).

effector memory T cells ($T_{em}$; CD45RA$^-$CCR7$^-$), naïve or naïve-like memory (CD45RA$^+$CCR7$^+$), and "terminally differentiated" effector memory T cells ($T_{emra}$; CD45RA$^+$CCR7$^-$)] that remained after heterologous Ad boosting. In contrast, the large expansion of HCV-specific T cells after MVA-NSmut boost was dominated by CD45RA$^-$ populations. The long-term memory population at the end of the study after heterologous Ad vaccination was predominantly lymph node homing (CCR7$^+$) T cells and that had reexpressed CD45RA; in contrast, after Ad/MVA regime, the dominant population were peripheral organ-homing (CCR7$^-$) $T_{em}$ with low expression of CD45RA (Fig. 5).

### An analysis of T cell functionality using CyTOF technology reveals the evolution of memory T cells over time

Single-cell mass cytometry (CyTOF) was used to produce an in-depth analysis of vaccine-induced HCV-specific T cells in two volunteers (319 and 322) at multiple time points. Antibodies labeled with heavy metal isotopes ($n$ = 35; table S2) that bind to surface and intracellular proteins allowed T cell phenotypes to be quantified. HCV-specific T cells were observed using metal-labeled peptide-MHC tetramers (gating strategy for CyTOF shown in fig. S8). Validating this approach, the expression of surface and intracellular markers measured by CyTOF correlated with those previously assessed using FACS (Spearman's rank $r$ = 0.8449, $P$ < 0.0001; fig. S9).

We assessed the overall potential for cytokine production of HCV-specific CD8$^+$ T cells after a 3-hour stimulation with phorbol 12-myristate 13-acetate (PMA)/ionomycin, so that the cytokine production by HCV-specific T cells could be compared to that of bulk CD8$^+$ T cells and avoid the rapid down-regulation of T cell receptor and subsequent lack of tetramer staining that accompanies peptide stimulation. Newell *et al.* (*30*) have previously shown that PMA/ionomycin stimulation induced comparable cytokine production by T cells to CD3/CD28 bead activation and that it allowed accurate multimer staining.

In keeping with the ICS data by FACS (fig. S5), we showed a progressive increase in HCV-specific CD8$^+$ T cells producing multiple cytokines over time (a feature not seen in the bulk CD8$^+$ population), with about 80% of cells having three or more functions by TW22 (14 weeks after MVA-NSmut; fig. S10). Evidence of a hierarchy of cytokine production by vaccine-induced HCV-specific T cells was observed, with single cytokine-producing CD8$^+$ T cells making MIP-1β (macrophage inflammatory protein 1β) and dual cytokine-producing T cells making MIP-1β and IFN-γ or TNFα, whereas granulocyte-macrophage colony-stimulating factor (GM-CSF) and IL-2 were only produced in

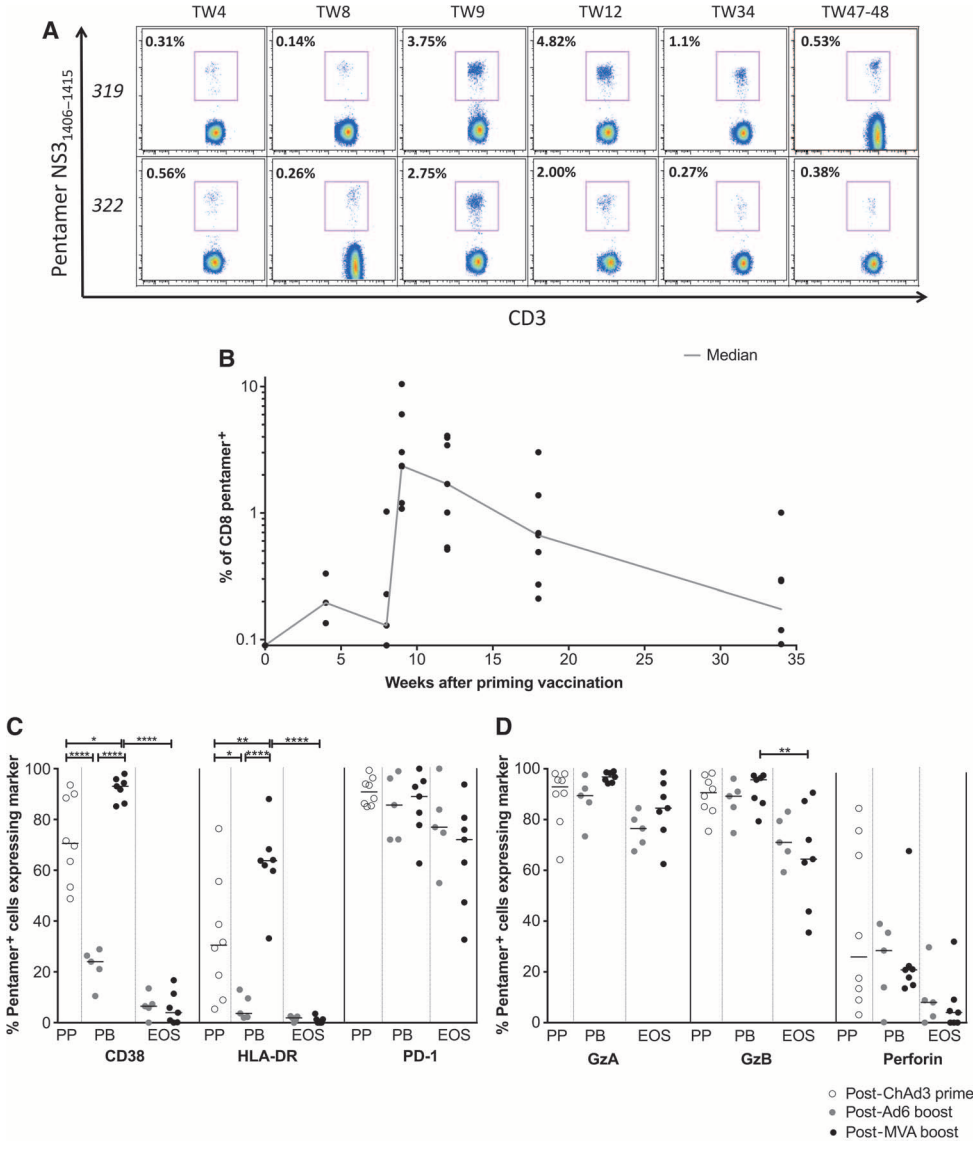


**Fig. 4. Phenotyping of vaccine-induced HCV-specific T cells.** (**A**) Example FACS plots of staining with tetramer A2–HCV $NS3_{1406–1415}$ in volunteers 319 and 322 (vaccinated with ChAd3-NSmut/MVA-NSmut) over the study time course. Gating is on live $CD3^+$ cells. Values indicate percentage of $CD8^+$ cell–binding pentamer. (**B**) Magnitude of pentamer cloud: The percentage of $CD8^+$ T cell–binding pentamer (HLA-A2–$HCV_{1406–1415}$ or HLA-A1–$HCV_{1435–1443}$) is shown for individual volunteers over the study time course. (**C** and **D**) Phenotype of vaccine-induced T cells: The percentage of the pentamer$^+$ cells expressing phenotypic markers CD38, HLA-DR, and PD-1 (C), or granzyme A (GzA), granzyme B (GzB), and perforin (D) are shown 4 weeks after ChAd3-NSmut prime [open circles; peak prime (PP)], after Ad6-NSmut boost [post-boost (PB), TW12; EOS, TW36; gray, $n$ = 5], and after MVA-NSmut boost (PB, TW9; EOS, TW34; black, $n$ = 7). Comparisons are made between vaccine regimens and between time points within a single regimen (ChAd3-NSmut/Ad6-NSmut versus ChAd3-NSmut/MVA-NSmut). Only statistically significant differences are shown. All pentamer staining and phenotyping were performed ex vivo without culture. Example FACS plots are shown in fig. S7.

combination with MIP-1β, IFN-γ, and TNFα by the most polyfunctional T cells (fig. S10).

To further analyze the CyTOF data, we used principal components analysis (PCA). The PCA was loaded with expression data from patient 319 at TW22, because this patient had the largest populations of "memory" $CD8^+$ T cells and a relatively large HCV-specific pentamer cloud (observed by FACS). Although this analysis is unsupervised, the apparent meaning of each component can be deduced on the basis of previously defined $CD8^+$ T cell subsets by looking at the markers that most influence the PCs (PC1: naïve versus memory, PC2: effector function, PC3: T cell differentiation status; Fig. 6, A to C). The first three PCs accounted for >50% of the variation within the data set (Fig. 6D), and therefore, these alone were plotted in PyMOL [three-dimensional PCA (3D-PCA)] to visualize $CD8^+$ T cell complexity. In theory, $CD8^+$ T cells could occupy any space within these plots; however, $CD8^+$ T cells clustered in defined, continuous regions, resulting in an "L-shaped" plot along the PC1-PC3 axis (Fig. 7). This pattern was observed in both individuals at all time points and in the two vaccine-naïve control patients.

We identified the location of classical and viral specific T cell subsets on this continuum before defining the location of the vaccine-induced HCV-specific T cells. Analysis of the relative expression of single markers (for example, IFN-γ, CD57, CD28, CD45RA, and CD27) showed that classical T cell subsets cluster in discrete niches (Fig. 7A and fig. S11). For example, the niche occupied by the naïve T cell population is easily identified by its high expression of CD45RA, CD27, and CD28 and low expression of IFN-γ, whereas most non-naïve (memory) T cells are positioned within an "L-shaped arm" that extends from the naïve population (Fig. 7A). The memory populations were further dissected through the analysis of CD45RA and CCR7, which showed that $T_{em}$, $T_{cm}$, and $T_{emra}$ occupied niches along the L-shaped arm (fig. S11). HCV, influenza, and CMV-specific tetramer$^+$ T cells were superimposed on the 3D-PCA plot of bulk CD8, showing that they also cluster in tightly restricted niches (Fig. 7B).

After ChAd3-NSmut prime (TW2) vaccination, HCV-specific T cells appear to occupy a niche close to the naïve population, in the area occupied by $T_{cm}$ ($CD45RA^-CCR7^+$) and FLU-specific T cells (Fig. 7B). After MVA-NSmut boost vaccination (TW9), the cells appear more heterogeneous and occupy a broader area across the continuum, with most HCV-specific T cells matching the position of $T_{em}$ and $CMV^+$ T cells in the 3D-PCA plots (Fig. 7B). At the latest time point studied, TW22, most HCV-specific T cells sit in a niche at the end of the L-shaped arm, in a similar location to $T_{emra}$ cells (Fig. 7B).

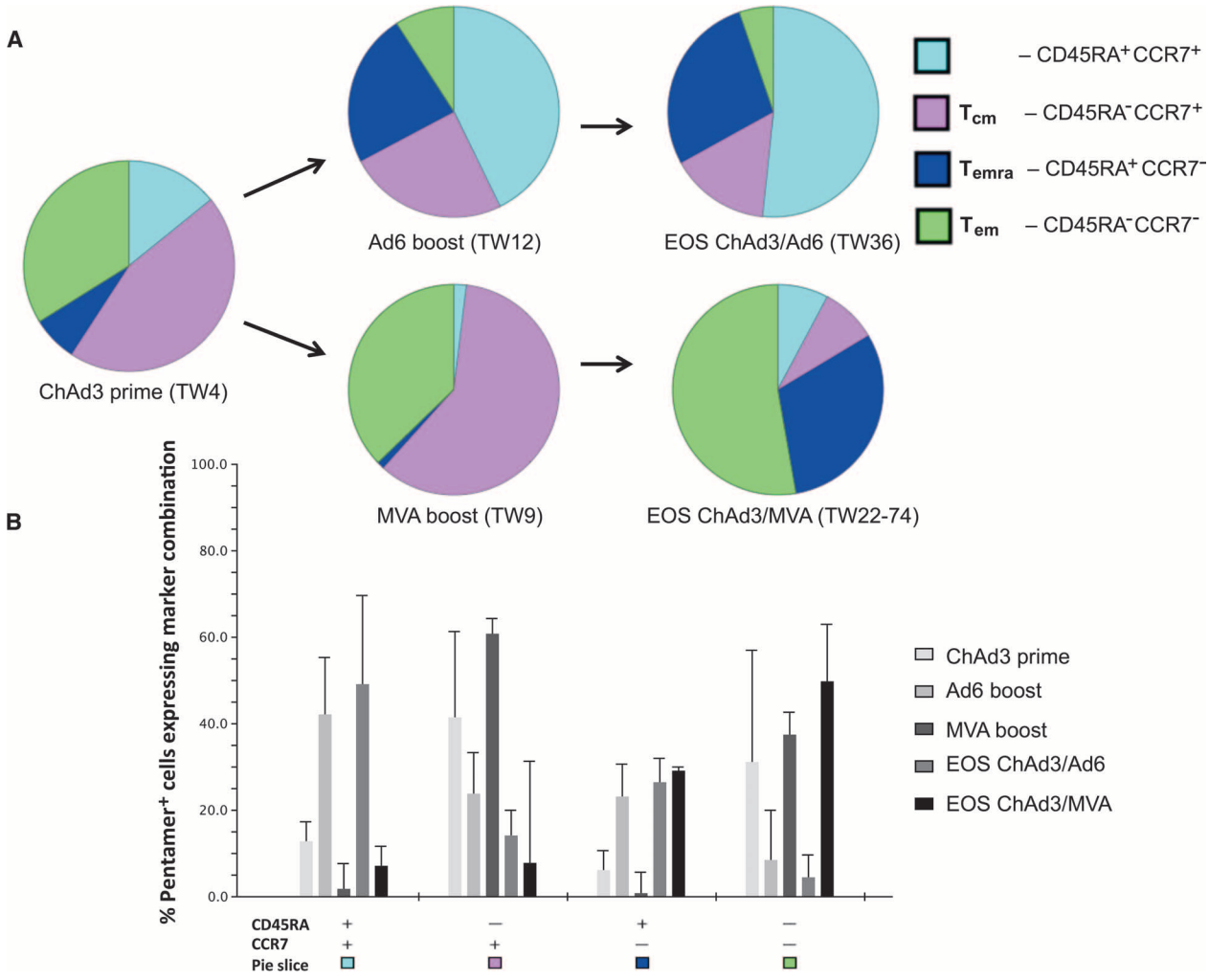


**Fig. 5. Memory phenotype of vaccine-induced CD8 T cells.** PBMCs were costained with pentamers to immunodominant epitopes in NS3 and with antibodies to human CD45RA and CCR7 ex vivo. Data are shown at the following time points: after ChAd3-NSmut prime (TW4, $n = 8$), peak after Ad6-NSmut boost (TW12, $n = 5$), at the end of the study after ChAd3-NSmut/Ad6-NSmut (TW36, $n = 5$; EOS ChAd3/Ad6), peak after MVA-NSmut boost (TW9, $n = 7$), and at the end of the study after ChAd3-NSmut/MVA-NSmut (TW22–74, $n = 7$; EOS ChAd3/MVA). (**A**) Pie charts show the proportion of the pentamer$^+$ cells, which display the naïve, $T_{em}$, $T_{emra}$, and $T_{cm}$ phenotype at the time points listed above. Pie base, median. (**B**) The bar graph shows the percentage of pentamer$^+$ cells displaying a particular phenotype at the time points listed above. Median and upper quartile are shown.

## DISCUSSION

We describe the development of a highly immunogenic T cell vaccine for HCV, using replication-defective chimpanzee Ad and MVA encoding the HCV NS proteins in a prime-boost strategy. This approach generates very high numbers of both CD4$^+$ and CD8$^+$ T cells, targeting multiple HCV antigens irrespective of host HLA background. Using established technologies and single-cell mass spectrometry (CyTOF), we show that T cells induced by vaccination are polyfunctional, that functionality increases over time, and that heterologous prime-boost with ChAd3 and MVA induced T cells with phenotypic and functional profiles distinct from those elicited by heterologous Ad vaccination. Furthermore, the strategy is simple, safe, and well tolerated in this phase 1 human study.

Whereas the correlates of protection in HCV are not precisely defined, studies of T cell immunity in natural infection suggest that a number of key parameters will be required. These include the targeting of multiple HCV antigens (*12*), the generation of CD4$^+$ and CD8$^+$ T cell subsets (*11*, *12*, *14*, *15*, *26*, *28*, *29*), the maintenance of a memory pool over time with the capacity to proliferate (*31*), and a population of circulating T cells with immediate effector function (*26*, *27*). A critical threshold for the magnitude of the T cell response required has not been established, although it is likely that in the context of a prophylactic vaccine, "more is better." The T cell vaccine regimen described here meets each of these criteria.

The magnitude of the HCV-specific T cell response generated by heterologous Ad-NSmut/MVA-NSmut vaccination is unprecedented. Priming with ChAd3-NSmut typically induced more than 1000 SFCs/$10^6$ PBMCs, whereas boosting with MVA-NSmut typically doubles this, with responses up to 7000 SFCs/$10^6$ PBMCs in some volunteers. The beneficial effect of MVA boosting is sustained overtime, with a clear elevation in the T cell "set point" and the maintenance of a sustained

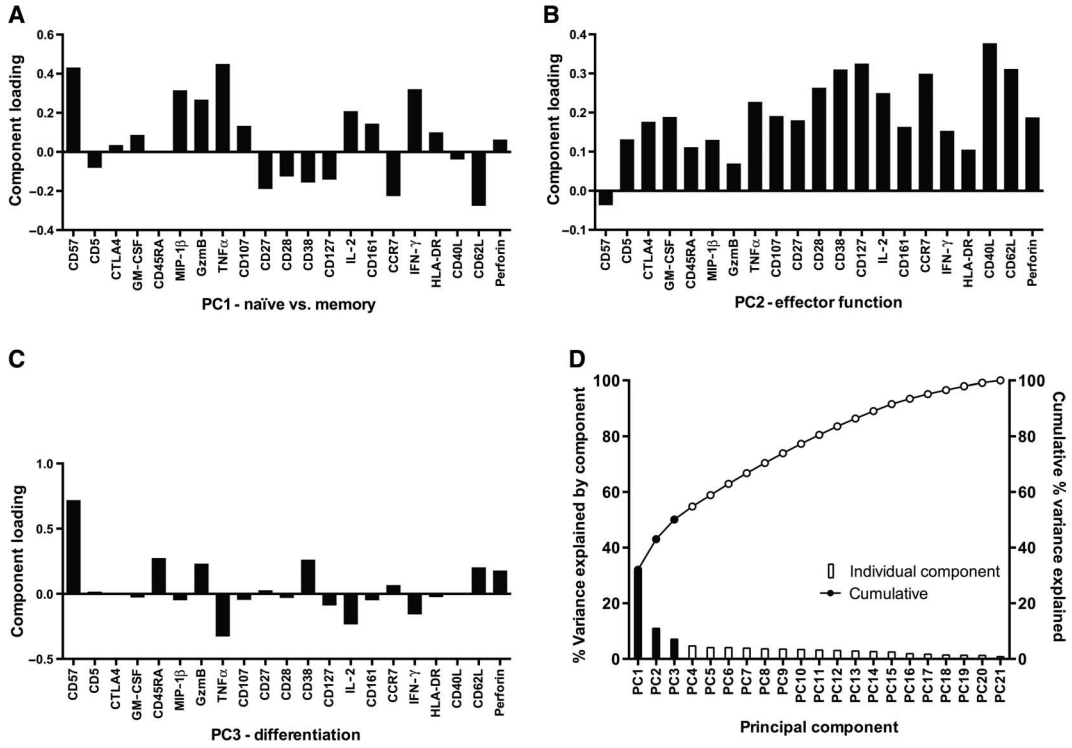


**Fig. 6. PCA of T cell immunity in human vaccinees.** The PCA was loaded with the relative expression of the markers listed on the *x* axis of the bar graphs above for all CD8$^+$ T cells from volunteer 319 at TW22. PCA produces summary variables/principal components that summarize as much variation in the expression of these markers across CD8 T cells as possible. The three components (PC1, PC2, and PC3) summarizing the most variation are shown with the weighting coefficients/component loading for each marker. (**D**) The percentage of the overall variation in the markers assayed on CD8 T cells explained by each principal component is plotted individually (bars) and cumulatively (line). The first three components, shown in (A) to (C) and used in the 3D-PCA plots in Fig. 7, are shown by filled bars/dots.

memory pool long term. Furthermore, all vaccinees respond to multiple HCV epitopes spanning the NS protein. The association of T cell breath with spontaneous viral resolution is controversial; some studies suggest that a T cell response against multiple NS antigens as measured by IFN-γ ELISpot is a predictor of viral clearance (*5*), whereas others have failed to demonstrate a clear association (*32*). Nevertheless, in the context of a prophylactic HCV vaccine, the generation of a broad antiviral response is likely to be important because HCV exists as quasispecies within an infected host and as distinct strains between individuals; targeting multiple HCV antigens increases the likelihood of vaccine-induced T cells recognizing incoming viral strains and escape variants.

Here, we could show that ChAd3/MVA vaccination induced T cell responses against all six NS antigenic pools in most individuals, and further mapping revealed as many as 31 different epitopes in a single vaccinee.

The ChAd3/MVA vaccination regimen is a significant improvement on the ChAd3/Ad6 regimen previously tested (*25*); a higher magnitude of T cell response is seen at all time points after boost vaccination, and both the breadth and proliferative capacity of the T cell response are significantly enhanced when measured immediately or long term after boost vaccination. The T cells induced by MVA boost vaccination have comparable cytolytic potential and polyfunctionality to those induced by heterologous Ad/Ad vaccination, but a distinct combination of T cell memory phenotypes is induced.

Because HCV exists as distinct genotypes that are broadly segregated geographically, we assessed the capacity of T cells generated by MVA boost encoding a subtype 1b immunogen to target genotypes 1a, 3a, and 4a. Although we have previously shown that T cell targets in genotypes 1 and 3 infection are distinct in the setting of natural infection (*33*), we find that in the context of a highly immunogenic vaccine, cross-reactive T cell responses between heterologous viral genotypes are readily generated but at a reduced magnitude. Whether these responses are sufficient to provide protection will require efficacy studies in mixed genotype populations.

Little is known about the ability of potent virally vectored vaccines to induce $T_{reg}$ subsets, which may influence vaccine efficacy. The induction of $T_{regs}$ has been associated with persistent infection in humans (*34*) and with repeated HCV antigen exposure in chimpanzees (*35*). $T_{reg}$ expansion in these studies may reflect priming of T cells in the tolerogenic liver environment, because we found no induction of $T_{regs}$ during vaccination with viral vectors encoding HCV antigens in the periphery.

CD4$^+$ T cell responses are known to play a central role in the generation of effective CD8$^+$ T cell immunity (*36*) and have been reproducibly associated with HCV viral control both in natural infection (*28*, *29*) and in chimpanzee challenge studies (*14*). Whereas heterologous boosting with MVA-NSmut markedly increased the magnitude of the CD8$^+$ T cell responses compared to heterologous Ad vaccination, the increase in the CD4$^+$ T cell response, producing IL-2, TNFα, and IFN-γ, was particularly striking. Furthermore, we show that the ability of this important T cell subset to secrete multiple cytokines is enhanced, and the capacity of CD4$^+$ T cells to proliferate increases over time after MVA-NSmut vaccination.

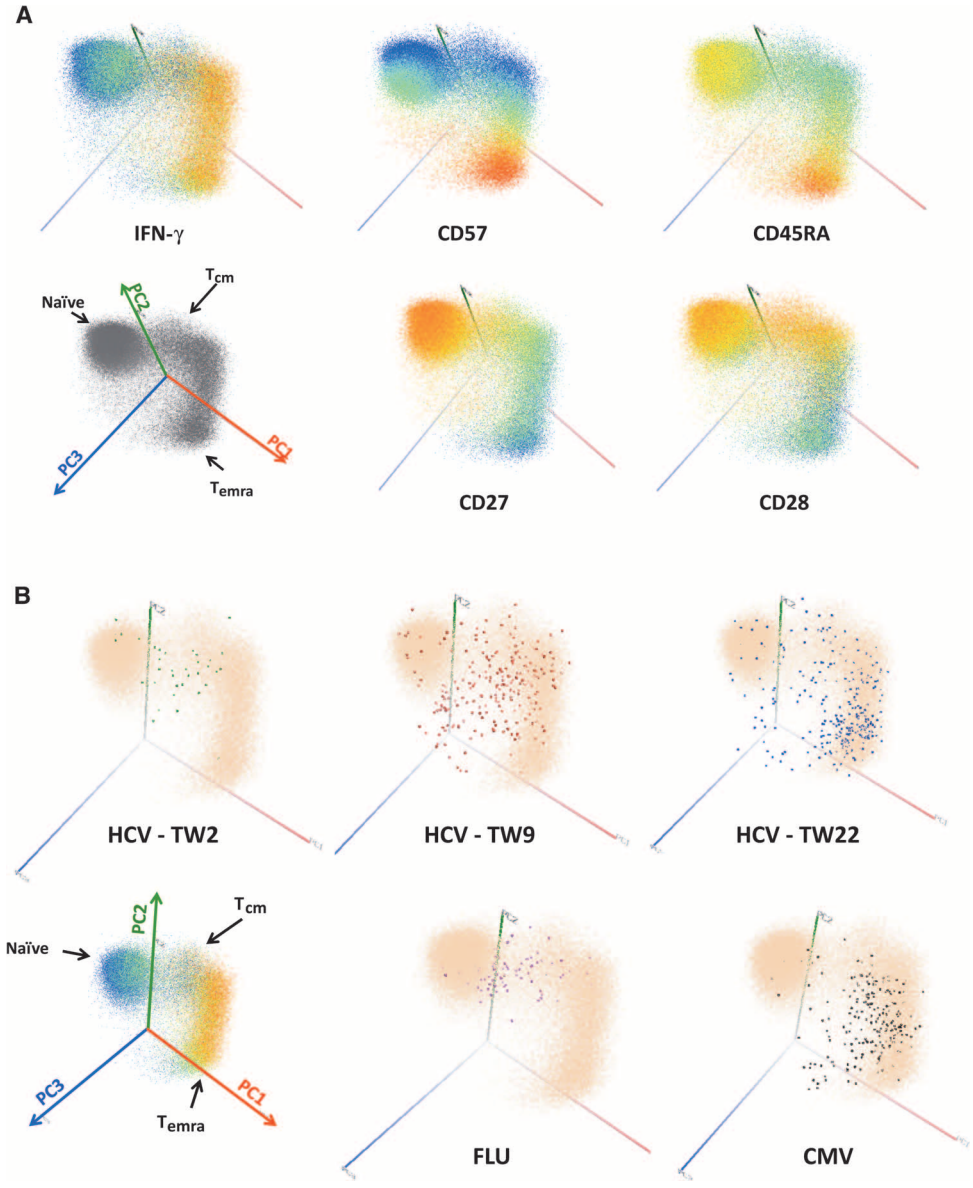


**Fig. 7. 3D-PCA of vaccine-induced CD8$^+$ T cells.** The first three principal components were plotted using the protein imaging program PyMOL (PC1 axis in red, PC2 axis in green, and PC3 axis in blue). (**A**) Bulk CD8 T cells. Each dot represents a single CD8 T cell, and in the images above, the cells are colored (blue, low; red, high) according to their relative expression within the CD8 population of IFN-γ, CD57, CD45RA, CD28, and CD27. A plot showing all CD8 T cells as gray dots shows the shape of the CD8 T cells in space according to the first three PCs with the relative locations of naïve, $T_{cm}$, and $T_{emra}$ populations highlighted by arrows. Data from volunteers 319 and 322. (**B**) 3D-PCA of vaccine-induced HCV-specific T cells: Each pink dot represents a single CD8$^+$ T cell (bulk CD8$^+$ T cells from 319 and 322) and plotted on the same axis are the tetramer$^+$ ($NS3_{1406–1415}$ HLA-A2) T cells at TW2 (peak after ChAd3-NSmut prime, green), at TW9 (peak after MVA-NSmut boost, red), and at TW22 (blue). The location of CMV (black)– and FLU (purple)–specific T cells, stained using tetramers on PBMCs from healthy unvaccinated volunteers (LC037 and LC046), are also shown. The bulk CD8$^+$ T cells are shown in the bottom left image, colored for their relative expression of IFN-γ with the locations of naïve, $T_{cm}$, and $T_{emra}$ populations highlighted by arrows for reference.

To increase the resolution of the functional and phenotypic assessment of vaccine-induced T cells, we used CyTOF. We show that there is a progressive increase in CD8 T cell polyfunctionality after MVA vaccination, and identified a clear hierarchy of cytokine production (MIP-1β > IFN-γ > IL-2). Evidence of a hierarchy in cytokine production has been previously described, whereby MIP-1β and IFN-γ are most readily released by T cells after limited stimulation, whereas IL-2 production is only triggered when a T cell has been exposed to high levels of antigen and costimulation (*30*, *37*, *38*).

Next, using both CyTOF and conventional flow cytometry, we characterized in detail the phenotype of HCV-specific T cells after Ad and MVA vaccination. Significant differences might be expected

because the vector for immunogen delivery exerts a profound influence on the type of T cell response elicited due to differences in innate signaling pathways and the persistence and quantity of antigen expressed (*39*, *40*). Low levels of transcriptionally active Ad have been shown to persist long term in both mice (*41*, *42*) and primates (*42*), whereas transgene expression by MVA becomes undetectable within a few days (*43*).

We find that the expression of markers of activation and cytolytic capacity are significantly greater after MVA boost. In addition, distinct combinations of T cell memory phenotypes are seen; after ChAd3 vaccination, CD45RA is strongly down-regulated, inducing dominant populations of $T_{cm}$ and $T_{em}$ cells. After heterologous Ad boost, the response is dominated by T cells with a "naïve"-like phenotype ($CD45RA^+CCR7^+$), even though these are functional antigen-experienced T cells. In contrast, after MVA-NSmut boost, there is a marked expansion of $T_{em}$ cells that increase further over time, so that by the end of the study, ~50% of cells are $T_{em}$, ~30% display a $T_{emra}$ phenotype, and ~10 to 15% appear to be $T_{cm}$ or naïve-like in phenotype. Through 3D-PCA analysis of the CyTOF data, we confirmed the previous observation that antigen-experienced cells exists along a continuum that extends from naïve toward memory populations, associated with a progressive loss of markers associated with naïve/early differentiated cells (CD28/CD27/CCR7) and a gain in expression of markers associated with senescence (CD57, CD45RA) (*30*). We show that vaccine-induced HCV-specific T cells cluster in restricted niches; after Ad priming, HCV-specific T cells cluster near the area occupied by influenza-specific and $T_{cm}$ $CD8^+$ T cells. In contrast, after MVA boost, these become more heterogeneous, occupying areas further along the differentiation pathway with a phenotype that is more typical of a CMV-specific T cell population.

This evolution of $CD8^+$ T cell memory is striking because a contraction toward a $T_{cm}$ phenotype might have been expected. Overall, the phenotype of T cells after Ad/MVA vaccination is remarkably similar to that induced by the highly efficacious yellow fever and smallpox (Dryvax) vaccines (that is, $T_{emra}/T_{em}$ phenotype and $PD\text{-}1^+$ expression), which are associated with lifelong protection (*44*). Furthermore, $T_{em}$ and $T_{emra}$ cell subsets have been associated with protection against HIV (*45*) and influenza (*46*) in natural history studies, and against simian immunodeficiency virus (*47*) and malaria (*48*) in vaccine studies. It is plausible that low-level persistence of Ad-derived transcripts contributes to the molding and maintenance of long-lived $T_{em}$ populations; recent data from studies of recombinant Ad vaccines in mice reveal long-term evolution of sustained $T_{em}$ populations, with a close resemblance to expanded $CD8^+$ T cell memory induced after CMV infection, and akin to those described here (*41*, *49*).

Although the diversity of the HCV genome represents a major challenge to vaccine development, a proportion of people infected with HCV are able to eradicate the virus spontaneously and effective T cell immunity appears to play a crucial role in this. Overall, we have generated a potent T cell vaccine that we believe may recapitulate and accelerate these events in vivo to prevent the development of chronic disease, thus paving the way for the first human efficacy studies. Suitable cohorts of IVDU populations have now been identified (*50*, *51*), and the first efficacy study of ChAd3-NSmut/MVA-NSmut in IVDUs has recently started in the United States (NCT01436357). This study will enable the assessment of vaccine immunogenicity, efficacy, and safety in a larger cohort of volunteers with a broad range of HLA types, exposed to different viral subtypes.

## MATERIALS AND METHODS

### Study design

The two primary endpoints in this study are safety and immunogenicity. The ChAd3-NSmut/MVA-NSmut vaccine study (HCV003) is registered in the ClinicalTrial.gov database (ID: NCT01296451). All volunteers gave written informed consent before enrolment, and the studies were conducted according to the principles of the Declaration of Helsinki and in accordance with Good Clinical Practice. Volunteers were recruited at the CCVTM (Centre for Clinical Vaccinology and Tropical Medicine), Churchill Hospital, Oxford. Vaccines were administered intramuscularly (ChAd3-NSmut dose, $2.5 \times 10^{10}$ vp; MVA-NSmut dose, $2 \times 10^8$ pfu). Volunteers were observed for 1 to 3 hours after vaccination. A dose escalation for ChAd3-NSmut is described in (*25*). The MVA dose was selected on the basis of the use of MVA vectors in human studies (*52*, *53*). Volunteers systematically documented all symptoms and recorded a daily oral temperature. Solicited and unsolicited local and systemic AEs were collected in diary cards and recorded in case report forms. A total of 24 volunteers were assessed for eligibility, and 15 volunteers were enrolled in one of two arms. Four individuals were enrolled into arm A1 and vaccinated with MVA-NSmut alone. Only after vaccine safety had been established in this arm were volunteers enrolled into arm A2. A total of 11 volunteers were enrolled into arm A2. One individual withdrew consent after receiving ChAd3-NSmut but before receiving MVA-NSmut. Hence, 10 volunteers completed the vaccine schedule in arm A2. One of these 10 individuals received a lower dose of ChAd3-NSmut because the required volume could not be extracted from the vaccine vial. Safety data from all 15 volunteers are reported; however, immunogenicity data are reported for all the A1 volunteers and the 9 volunteers in arm A2 who completed the vaccination schedule with the doses stated above. An additional two volunteers vaccinated with the arm A2 schedule were subsequently included for assessment of $T_{reg}$ subsets only (fig. S3). Both exposure to HCV (defined as HCV antibody and HCV RNA positivity) and recent intravenous drug use were study exclusion criteria. HCV antibodies, quantitative HCV RNA, and T cell response to HCV antigens were all undetectable at baseline. There were no signs or symptoms of viral hepatitis or an increase in liver enzymes during the study.

Comparisons are made with the previously published ChAd3-NSmut/Ad6-NSmut vaccine study (HCV001; group 10 ChAd3-NSmut dose, $2.5 \times 10^{10}$ vp; group 11 ChAd3-NSmut dose, $7.5 \times 10^{10}$ vp; doses were combined for analysis because we have previously shown that there is no dose effect above $2.5 \times 10^{10}$ vp) registered as ID NCT01070407 [$n = 9$; safety data and immunology previously published (*25*)]. Study groups and vaccination regimes in studies HCV001 and HCV003 are detailed in table S1.

### Ad constructs

The Ad6 and ChAd3 vectors encoding the NS3–5B region (1985 amino acids) of genotype 1b BK strain (based on sequence accession number M58335) have been described previously (*20*, *22*) and were manufactured at the Clinical BioManufacturing Facility, Oxford University.

### Generation of the MVA-NS

The NSmut expression cassette was subcloned into the MVA shuttle vector pMVA-GFP-TD flanked by TKL (thymidine kinase gene left region) and TKR (thymidine kinase gene right region) generating

the transfer vector pMVA-GFP-TD-NSmut. pMVA-GFP-TD-NSmut drives the antigen expression using the vaccinia P7.5 early/late promoter and expression of green fluorescent protein (GFP) using the fowlpox late promoter FP4b. The production of the recombinant MVA-NSmut virus was based on in vivo recombination between the MVA–Red genome and homologous sequence (TKL and TKR) within the transfer vector pMVA-GFP-TD-NSmut. Polymerase chain reaction was performed to check for the presence of NS transgene and the absence of wild-type MVA and MVA–Red virus.

### Peptides and antigens

A set of 494 peptides, 15 amino acids in length, overlapping by 11 amino acids and spanning the open reading frame from NS3 to NS5B (1985 amino acids) of HCV genotype 1b strain BK (matching the vaccine immunogen) were obtained from BEI Resources. Peptides were initially dissolved in DMSO and arranged into six pools labeled F to M and corresponding respectively to NS3p, NS3h, NS4, NS5A, NS5B I, and NS5B II (mean, 82; range, 73 to 112 peptides per pool). Pools were used with each single peptide at a final concentration of 3 or 1 μg/ml in ELISpot and ICS assays, respectively. For cross-reactivity experiments, similar peptide pools derived from HCV genotype 1a (H77 strain), genotype 3a (GenBank accession D28917), and genotype 4a (ED43; EMBL accession Y11604) were prepared identically. Optimal length peptides were purchased from ProImmune Ltd.

### ELISpot assays

Ex vivo IFN-γ ELISpot assays were performed as described previously on freshly isolated PBMCs plated in triplicate at $2 \times 10^5$ PBMCs per well (*25*). A robust positive cutoff was previously calculated from 74 healthy HCV seronegative volunteers. For a positive response, the mean of antigen wells was determined (i) to be greater than 48 SFCs/$10^6$ PBMCs (mean + 3 SDs) and (ii) to exceed 3× background. Background wells (medium only, cells + DMSO) were typically zero to four spots. Internal positive controls included concanavalin A, FEC (mixed HLA class–I restricted peptides from FLU, EBV, and CMV), and a CMV lysate. Total NS response was calculated by summing responses to all positive pools (NS3p–NS5B II) and corrected for background.

Cells were counted using a Guava Personal Cell Analysis system (Merck Millipore) as previously described (*25*).

### Proliferation assays

Ex vivo proliferation assays were performed on freshly isolated PBMCs plated in triplicate at $2 \times 10^5$ PBMCs per well using conventional [$^3$H]thymidine incorporation methods and HCV proteins (1 μg/ml) as described previously (*25*). Data are displayed as SI (fold change above background). A positive response is defined as SI ≥3.

### Intracellular cytokine staining

ICS was performed as described previously (*25*) on fresh or thawed PBMCs after 3 hours of resting at room temperature. Briefly, PBMCs were stimulated using peptides in pool combinations (F + G + H = NS3–4, I + L + M = NS5A–B, 1 μg/ml) or with individual pools, peptides (15 mers and optimal 8 mers, 1 μg/ml), unstimulated (controlled for DMSO), or PMA/ionomycin (50 and 500 ng/ml, respectively). After overnight stimulation (brefeldin A was added after 1 hour at 10 μg/ml), cells were stained with LIVE/DEAD Fixable Near-IR Dead Cell Stain Kit (Invitrogen; used in all FACS assays), fixed (1% paraformaldehyde), permeabilized (eBioscience 10× perm buffer), and stained with the following antibodies: CD3–PO (Pacific Orange), CD4–Qdot 605, CD8–PerCP (peridinin chlorophyll protein)–Cy5.5, IFN-γ–Alexa Fluor 700, IL-2–APC (allophycocyanin), and TNFα–PE (phycoerythrin)–Cy7 (table S2).

For analysis of peptide-specific function, PBMCs were stimulated with peptide at 1 μg/ml or control DMSO or PMA/ionomycin. ICS was then performed as described above and stained with the following antibodies: CD3-PO, CD4–Qdot 605, CD8–PB (Pacific Blue), IFN-γ–Alexa Fluor 700, IL-2–APC, TNFα-PE-Cy7, and MIP-1β–PE (table S2).

Flow cytometry was performed using a BD LSRII and analysis by FlowJo (Tree Star). Analysis of polyfunctionality was performed using Pestle and SPICE version 5.3, downloaded from http://exon.niaid.nih.gov (*54*). All ICS data are corrected for background.

### Pentamer and $T_{reg}$ staining, short-term cell lines, and flow cytometry

PE-labeled pentamers loaded with HCV $NS3_{1406–1415}$ (KLSALGINAV; HLA-A*0201) or HCV $NS3_{1435–1443}$ (ATDALMTGY, HLA-A*0101) were obtained from ProImmune (table S2 for list of antibodies and fluorochromes costained with pentamers). The specificity of pentamers was tested on HLA-matched prevaccination samples from healthy volunteers (*25*).

Pentamers were centrifuged at 4°C (1400*g*, 10 min), and 1 μl was taken from the supernatant and used to stain $1 \times 10^6$ to $2 \times 10^6$ fresh or thawed PBMCs in 50 μl of phosphate-buffered saline. PBMCs were then sequentially stained with fixable NIR LIVE/DEAD stain, fixed (1% paraformaldehyde), permeabilized (for internal stains only; eBioscience 10× perm buffer), and then stained with surface or internal antibody cocktails separately for 30 min. Fluorescent markers were observed and analyzed using a BD LSRII and FlowJo software (Tree Star). CD45RA/CCR7 subsets were analyzed using Pestle and SPICE. Fluorescence minus one (FMO) samples were performed using a CMV pentamer on $CMV^+$ PBMCs, and fixed gating strategies were used throughout.

For quantification of $T_{reg}$ subsets, frozen PBMCs were thawed and stained with fixable NIR LIVE/DEAD stain, surface-stained with CD3-PO, CD4–Qdot 605, CD25-PE-Cy7, CD8-PB, and CD127-APC antibodies, then fixed, permeabilized, and stained with FoxP3–Alexa Fluor 700 according to eBioscience One-step protocol for intracellular (nuclear) proteins using the Foxp3/Transcription Factor Staining Buffer Set (catalog no. 00-5523-00).

### Mass cytometry using CyTOF

T cell phenotype and function were determined by mass cytometry analysis in volunteers 319 and 322 at TW2/4 (peak T cell immunogenicity after ChAd3-NSmut vaccination), TW9 (peak T cell immunogenicity after MVA-NSmut vaccination), and TW22, performed on frozen PBMCs.

Detailed methodology is described elsewhere (*30*). Briefly, cryopreserved cells were thawed and left overnight at 37°C. Dead cells were then removed by Ficoll density separation. For stimulation, cells were cultured for 3 hours with PMA (150 ng/ml) + 1 mM ionomycin in the presence of brefeldin A, monensin, and anti-CD107α/β. Cells were then stained with a cocktail of metal-conjugated surface antibodies ($n$ = 35) and tetramers ($n$ = 3; table S2). Cells were fixed, left overnight, and then permeabilized and stained with metal-conjugated antibodies for intracellular markers and with DNA interchelators (iridium, DVS Sciences).

Purified antibodies were labeled with heavy metal–preloaded maleimide-coupled MAXPAR chelating polymers via the "Pre-Load Method v1.1" as previously described (*30*). Cells were also stained with three fluorochrome-labeled flow antibodies [CD161-APC, γδ–FITC (fluorescein isothiocyanate), and PD-1–PE] and then stained for anti-PE, anti-APC, and anti-FITC antibodies conjugated to metals. CD3 was stained using a Qdot antibody, which is composed of cadmium.

Tetramer generation was performed as previously described (*55*). Briefly, HLA-A*0201 MHC molecules folded with ultraviolet (UV)–cleavable peptides were biotinylated and purified. Peptides were exchanged by UV irradiation of MHC in the presence of high concentrations of CMV $pp65_{482–490}$ NLVPMVATV, FLU $M1/MP_{58–66}$ GILGFVFTL, and HCV $NS3_{1405–1415}$ KLSALGINAV. pMHC molecules were then tetramerized and labeled with heavy metal isotopes coupled to streptavidin. Tetramers were multiplexed by conjugating each tetramer to an exclusive combinations of two heavy metals for each tetramer-peptide specificity (table S2) (*56*). Data were acquired and analyzed on the CyTOF machine as previously described (*30*). The specificity of tetramers was tested on PBMCs from two HLA-matched unvaccinated individuals.

### Mass cytometry data analysis

Built-in cell-identifying software on the CyTOF creates an FCS file, enabling mass cytometry data to be analyzed in a manner similar to standard flow cytometry data by FlowJo software (Tree Star Inc.).

For PCA, cells were gated on live $CD3^+CD8^+$ T cells (principal component loaded using data from patient 319 at TW22 and then applied to the other data sets), and these events were exported to a tab-delimited text file with FlowJo v9.3.2 for further analysis with scripts written in MATLAB. FCS files containing these additional parameters were created using a custom algorithm written in Java (text to FCS script provided by W. Moore). pdb files were also created using MATLAB that could be read by PyMOL software (DeLano Scientific LLC). All MATLAB scripts started with transformation of data into logicle biexponential scaling as described (*30*).

### Statistical analysis

Nonparametric tests were used throughout, paired for within-individual comparisons (Wilcoxon) and unpaired for group comparisons (Mann-Whitney). For correlations, a nonparametric test was used (Spearman). For multiple comparisons, a one-way ANOVA with Bonferroni correction was used. Prism (v6.0 for Mac) was used throughout. $^*P \leq 0.05$; $^{**}P \leq 0.01$; $^{***}P \leq 0.001$; $^{****}P < 0.0001$. Only statistically significant results are reported in figures.

## SUPPLEMENTARY MATERIALS

www.sciencetranslationalmedicine.org/cgi/content/full/6/261/261ra153/DC1

Fig. S1. Safety data after vaccination.
Fig. S2. Magnitude of FLU-, EBV-, and CMV-specific T cell responses across the vaccine trial.
Fig. S3. CD4 $T_{regs}$ across vaccine trial.
Fig. S4. Breadth of cross-reactive T cell responses to genotype 1a, 3a, and 4a peptides.
Fig. S5. Polyfunctionality of HCV-specific $CD4^+$ and $CD8^+$ T cells in volunteers receiving ChAd3-NSmut/MVA-NSmut vaccination.
Fig. S6. Polyfunctional cells make more cytokine per cell than do monofunctional cells.
Fig. S7. Gating strategy for fluorescence cytometry.
Fig. S8. Gating strategy for mass cytometry.
Fig. S9. A correlation between measurements of phenotypic markers on T cells by FACS versus by CyTOF.
Fig. S10. Polyfunctionality of HCV-specific CD8 T cells analyzed by CyTOF.
Fig. S11. Plotting T cell memory subsets against principal components.
Table S1. Study design and trial groups.
Table S2. List of antibodies and markers used in CyTOF and FACS staining panels.
Table S3. Magnitude of T cell responses to HCV NS after MVA prime vaccination.
Table S4. Proliferative capacity of T cells after boost vaccination.

## REFERENCES AND NOTES


1. G. M. Lauer, B. D. Walker, Hepatitis C virus infection. *N. Engl. J. Med.* **345**, 41–52 (2001).
2. W. N. Schmidt, D. R. Nelson, J. M. Pawlotsky, K. E. Sherman, D. L. Thomas, R. T. Chung, Direct-acting antiviral agents and the path to interferon independence. *Clin. Gastroenterol. Hepatol.* **12**, 728–737 (2014).
3. E. J. Gane, K. Agarwal, Directly acting antivirals (DAAs) for the treatment of chronic hepatitis C virus infection in liver transplant patients: "A flood of opportunity". *Am. J. Transplant.* **14**, 994–1002 (2014).
4. P. Y. Kwo, E. J. Lawitz, J. McCone, E. R. Schiff, J. M. Vierling, D. Pound, M. N. Davis, J. S. Galati, S. C. Gordon, N. Ravendhran, L. Rossaro, F. H. Anderson, I. M. Jacobson, R. Rubin, K. Koury, L. D. Pedicone, C. A. Brass, E. Chaudhri, J. K. Albrecht; SPRINT-1 investigators, Efficacy of boceprevir, an NS3 protease inhibitor, in combination with peginterferon alfa-2b and ribavirin in treatment-naive patients with genotype 1 hepatitis C infection (SPRINT-1): An open-label, randomised, multicentre phase 2 trial. *Lancet* **376**, 705–716 (2010).
5. E. Spada, A. Mele, A. Berton, L. Ruggeri, L. Ferrigno, A. R. Garbuglia, M. P. Perrone, G. Girelli, P. Del Porto, E. Piccolella, M. U. Mondelli, P. Amoroso, R. Cortese, A. Nicosia, A. Vitelli, A. Folgori, Multispecific T cell response and negative HCV RNA tests during acute HCV infection are early prognostic factors of spontaneous clearance. *Gut* **53**, 1673–1681 (2004).
6. L. Swadling, P. Klenerman, E. Barnes, Ever closer to a prophylactic vaccine for HCV. *Expert Opin. Biol. Ther.* **13**, 1109–1124 (2013).
7. K. Fitzmaurice, D. Petrovic, N. Ramamurthy, R. Simmons, S. Merani, S. Gaudieri, S. Sims, E. Dempsey, E. Freitas, S. Lea, S. McKiernan, S. Norris, A. Long, D. Kelleher, P. Klenerman, Molecular footprints reveal the impact of the protective HLA-A*03 allele in hepatitis C virus infection. *Gut* **60**, 1563–1571 (2011).
8. C. Neumann-Haefelin, R. Thimme, Impact of the genetic restriction of virus-specific T-cell responses in hepatitis C virus infection. *Genes Immun.* **8**, 181–192 (2007).
9. A. Y. Kim, T. Kuntzen, J. Timm, B. E. Nolan, M. A. Baca, L. L. Reyor, A. C. Berical, A. J. Feller, K. L. Johnson, J. Schulze zur Wiesch, G. K. Robbins, R. T. Chung, B. D. Walker, M. Carrington, T. M. Allen, G. M. Lauer, Spontaneous control of HCV is associated with expression of *HLA-B*57* and preservation of targeted epitopes. *Gastroenterology* **140**, 686–696 (2011).
10. P. Duggal, C. L. Thio, G. L. Wojcik, J. J. Goedert, A. Mangia, R. Latanich, A. Y. Kim, G. M. Lauer, R. T. Chung, M. G. Peters, G. D. Kirk, S. H. Mehta, A. L. Cox, S. I. Khakoo, L. Alric, M. E. Cramp, S. M. Donfield, B. R. Edlin, L. H. Tobler, M. P. Busch, G. Alexander, H. R. Rosen, X. Gao, M. Abdel-Hamid, R. Apps, M. Carrington, D. L. Thomas, Genome-wide association study of spontaneous resolution of hepatitis C virus infection: Data from multiple cohorts. *Ann. Intern. Med.* **158**, 235–245 (2013).
11. F. Lechner, D. K. Wong, P. R. Dunbar, R. Chapman, R. T. Chung, P. Dohrenwend, G. Robbins, R. Phillips, P. Klenerman, B. D. Walker, Analysis of successful immune responses in persons infected with hepatitis C virus. *J. Exp. Med.* **191**, 1499–1512 (2000).
12. G. M. Lauer, E. Barnes, M. Lucas, J. Timm, K. Ouchi, A. Y. Kim, C. L. Day, G. K. Robbins, D. R. Casson, M. Reiser, G. Dusheiko, T. M. Allen, R. T. Chung, B. D. Walker, P. Klenerman, High resolution analysis of cellular immune responses in resolved and persistent hepatitis C virus infection. *Gastroenterology* **127**, 924–936 (2004).
13. N. H. Shoukry, A. Grakoui, M. Houghton, D. Y. Chien, J. Ghrayeb, K. A. Reimann, C. M. Walker, Memory $CD8^+$ T cells are required for protection from persistent hepatitis C virus infection. *J. Exp. Med.* **197**, 1645–1655 (2003).
14. A. Grakoui, N. H. Shoukry, D. J. Woollard, J. H. Han, H. L. Hanson, J. Ghrayeb, K. K. Murthy, C. M. Rice, C. M. Walker, HCV persistence and immune evasion in the absence of memory T cell help. *Science* **302**, 659–662 (2003).
15. W. O. Osburn, B. E. Fisher, K. A. Dowd, G. Urban, L. Liu, S. C. Ray, D. L. Thomas, A. L. Cox, Spontaneous control of primary hepatitis C virus infection and immunity against persistent reinfection. *Gastroenterology* **138**, 315–324 (2010).
16. E. Giang, M. Dorner, J. C. Prentoe, M. Dreux, M. J. Evans, J. Bukh, C. M. Rice, A. Ploss, D. R. Burton, M. Law, Human broadly neutralizing antibodies to the envelope glycoprotein complex of hepatitis C virus. *Proc. Natl. Acad. Sci. U.S.A.* **109**, 6205–6210 (2012).
17. J. M. Pestka, M. B. Zeisel, E. Bläser, P. Schürmann, B. Bartosch, F. L. Cosset, A. H. Patel, H. Meisel, J. Baumert, S. Viazov, Rapid induction of virus-neutralizing antibodies and viral clearance in a single-source outbreak of hepatitis C. *Proc. Natl. Acad. Sci. U.S.A.* **104**, 6025–6030 (2007).
18. M. Houghton, S. Abrignani, Prospects for a vaccine against the hepatitis C virus. *Nature* **436**, 961–966 (2005).
19. J. L. Law, C. Chen, J. Wong, D. Hockman, D. M. Santer, S. E. Frey, R. B. Belshe, T. Wakita, J. Bukh, C. T. Jones, C. M. Rice, S. Abrignani, D. L. Tyrrell, M. Houghton, A hepatitis C virus (HCV) vaccine comprising envelope glycoproteins gpE1/gpE2 derived from a single isolate elicits broad cross-genotype neutralizing antibodies in humans. *PLOS One* **8**, e59776 (2013).

20. A. Folgori, S. Capone, L. Ruggeri, A. Meola, E. Sporeno, B. B. Ercole, M. Pezzanera, R. Tafi, M. Arcuri, E. Fattori, A. Lahm, A. Luzzago, A. Vitelli, S. Colloca, R. Cortese, A. Nicosia, A T-cell HCV vaccine eliciting effective immunity against heterologous virus challenge in chimpanzees. *Nat. Med.* **12**, 190–197 (2006).
21. S. P. Buchbinder, D. V. Mehrotra, A. Duerr, D. W. Fitzgerald, R. Mogg, D. Li, P. B. Gilbert, J. R. Lama, M. Marmor, C. del Rio, M. J. McElrath, D. R. Casimiro, K. M. Gottesdiener, J. A. Chodakewitz, L. Corey, M. N. Robertson; Step Study Protocol Team, Efficacy assessment of a cell-mediated immunity HIV-1 vaccine (the Step Study): A double-blind, randomised, placebo-controlled, test-of-concept trial. *Lancet* **372**, 1881–1893 (2008).
22. S. Colloca, E. Barnes, A. Folgori, V. Ammendola, S. Capone, A. Cirillo, L. Siani, M. Naddeo, F. Grazioli, M. L. Esposito, M. Ambrosio, A. Sparacino, M. Bartiromo, A. Meola, K. Smith, A. Kurioka, G. A. O'Hara, K. J. Ewer, N. Anagnostou, C. Bliss, A. V. S. Hill, C. Traboni, P. Klenerman, R. Cortese, A. Nicosia, Vaccine vectors derived from a large collection of simian adenoviruses induce potent cellular immunity across multiple species. *Sci. Transl. Med.* **4**, 115ra2 (2012).
23. S. Capone, A. M. D'Alise, V. Ammendola, S. Colloca, R. Cortese, A. Nicosia, A. Folgori, Development of chimpanzee adenoviruses as vaccine vectors: Challenges and successes emerging from clinical trials. *Expert Rev. Vaccines* **12**, 379–393 (2013).
24. S. Capone, I. Zampaglione, A. Vitelli, M. Pezzanera, L. Kierstead, J. Burns, L. Ruggeri, M. Arcuri, M. Cappelletti, A. Meola, B. B. Ercole, R. Tafi, C. Santini, A. Luzzago, T. M. Fu, S. Colloca, G. Ciliberto, R. Cortese, A. Nicosia, E. Fattori, A. Folgori, Modulation of the immune response induced by gene electrotransfer of a hepatitis C virus DNA vaccine in nonhuman primates. *J. Immunol.* **177**, 7462–7471 (2006).
25. E. Barnes, A. Folgori, S. Capone, L. Swadling, S. Aston, A. Kurioka, J. Meyer, R. Huddart, K. Smith, R. Townsend, A. Brown, R. Antrobus, V. Ammendola, M. Naddeo, G. O'Hara, C. Willberg, A. Harrison, F. Grazioli, M. L. Esposito, L. Siani, C. Traboni, Y. Oo, D. Adams, A. Hill, S. Colloca, A. Nicosia, R. Cortese, P. Klenerman, Novel adenovirus-based vaccines induce broad and sustained T cell responses to HCV in man. *Sci. Transl. Med.* **4**, 115ra1 (2012).
26. S. Urbani, B. Amadei, P. Fisicaro, D. Tola, A. Orlandini, L. Sacchelli, C. Mori, G. Missale, C. Ferrari, Outcome of acute hepatitis C is related to virus-specific CD4 function and maturation of antiviral memory CD8 responses. *Hepatology* **44**, 126–139 (2006).
27. A. A. Takaki, M. M. Wiese, G. G. Maertens, E. E. Depla, U. U. Seifert, A. A. Liebetrau, J. L. J. Miller, M. P. M. Manns, B. B. Rehermann, Cellular immune responses persist and humoral responses decrease two decades after recovery from a single-source outbreak of hepatitis C. *Nat. Med.* **6**, 578–582 (2000).
28. J. T. Gerlach, H. M. Diepolder, M. C. Jung, N. H. Gruener, W. W. Schraut, R. Zachoval, R. Hoffmann, C. A. Schirren, T. Santantonio, G. R. Pape, Recurrence of hepatitis C virus after loss of virus-specific $CD4^+$ T-cell response in acute hepatitis C. *Gastroenterology* **117**, 933–941 (1999).
29. R. Thimme, D. Oldach, K. M. Chang, C. Steiger, S. C. Ray, F. V. Chisari, Determinants of viral clearance and persistence during acute hepatitis C virus infection. *J. Exp. Med.* **194**, 1395–1406 (2001).
30. E. W. Newell, N. Sigal, S. C. Bendall, G. P. Nolan, M. M. Davis, Cytometry by time-of-flight shows combinatorial cytokine expression and virus-specific cell niches within a continuum of $CD8^+$ T cell phenotypes. *Immunity* **36**, 142–152 (2012).
31. A. Folgori, E. Spada, M. Pezzanera, L. Ruggeri, A. Mele, A. R. Garbuglia, M. P. Perrone, P. Del Porto, E. Piccolella, R. Cortese, A. Nicosia, A. Vitelli; Acute Hepatitis C Italian Study Group, Early impairment of hepatitis C virus specific T cell proliferation during acute infection leads to failure of viral clearance. *Gut* **55**, 1012–1019 (2006).
32. G. M. Lauer, M. Lucas, J. Timm, K. Ouchi, A. Y. Kim, C. L. Day, J. Schulze Zur Wiesch, G. Paranhos-Baccala, I. Sheridan, D. R. Casson, M. Reiser, R. T. Gandhi, B. Li, T. M. Allen, R. T. Chung, P. Klenerman, B. D. Walker, Full-breadth analysis of $CD8^+$ T-cell responses in acute hepatitis C virus infection and early therapy. *J. Virol.* **79**, 12979–12988 (2005).
33. I. S. Humphreys, A. von Delft, A. Brown, L. Hibbert, J. D. Collier, G. R. Foster, M. Rahman, A. Christian, P. Klenerman, E. Barnes, HCV genotype-3a T cell immunity: Specificity, function and impact of therapy. *Gut* **61**, 1589–1599 (2012).
34. S. M. Ward, B. C. Fox, P. J. Brown, J. Worthington, S. B. Fox, R. W. Chapman, K. A. Fleming, A. H. Banham, P. Klenerman, Quantification and localisation of FOXP3+ T lymphocytes and relation to hepatic inflammation during chronic HCV infection. *J. Hepatol.* **47**, 316–324 (2007).
35. S. H. Park, N. S. Veerapu, E. C. Shin, A. Biancotto, J. P. McCoy, S. Capone, A. Folgori, B. Rehermann, Subinfectious hepatitis C virus exposures suppress T cell responses against subsequent acute infection. *Nat. Med.* **19**, 1638–1642 (2013).
36. A. J. Zajac, J. N. Blattman, K. Murali-Krishna, D. J. Sourdive, M. Suresh, J. D. Altman, R. Ahmed, Viral immune evasion due to persistence of activated T cells without effector function. *J. Exp. Med.* **188**, 2205–2213 (1998).
37. N. L. La Gruta, S. J. Turner, P. C. Doherty, Hierarchies in cytokine expression profiles for acute and resolving influenza virus-specific $CD8^+$ T cell responses: Correlation of cytokine profile and TCR avidity. *J. Immunol.* **172**, 5553–5560 (2004).
38. A. Viola, A. Lanzavecchia, T cell activation determined by T cell receptor number and tunable thresholds. *Science* **273**, 104–106 (1996).
39. D. R. Casimiro, L. Chen, T. M. Fu, R. K. Evans, M. J. Caulfield, M. E. Davies, A. Tang, M. Chen, L. Huang, V. Harris, D. C. Freed, K. A. Wilson, S. Dubey, D. M. Zhu, D. Nawrocki, H. Mach, R. Troutman, L. Isopi, D. Williams, W. Hurni, Z. Xu, J. G. Smith, S. Wang, X. Liu, L. Guan, R. Long, W. Trigona, G. J. Heidecker, H. C. Perry, N. Persaud, T. J. Toner, Q. Su, X. Liang, R. Youil, M. Chastain, A. J. Bett, D. B. Volkin, E. A. Emini, J. W. Shiver, Comparative immunogenicity in rhesus monkeys of DNA plasmid, recombinant vaccinia virus, and replication-defective adenovirus vectors expressing a human immunodeficiency virus type 1 gag gene. *J. Virol.* **77**, 6305–6313 (2003).
40. L. Flatz, R. Roychoudhuri, M. Honda, A. Filali-Mouhim, J. P. Goulet, N. Kettaf, M. Lin, M. Roederer, E. K. Haddad, R. P. Sékaly, G. J. Nabel, Single-cell gene-expression profiling reveals qualitatively distinct CD8 T cells elicited by different gene-based vaccines. *Proc. Natl. Acad. Sci. U.S.A.* **108**, 5724–5729 (2011).
41. B. Bolinger, S. Sims, G. O'Hara, C. de Lara, E. Tchilian, S. Firner, D. Engeler, B. Ludewig, P. Klenerman, A new model for $CD8^+$ T cell memory inflation based upon a recombinant adenoviral vector. *J. Immunol.* **190**, 4162–4174 (2013).
42. N. Tatsis, J. C. Fitzgerald, A. Reyes-Sandoval, K. C. Harris-McCoy, S. E. Hensley, D. Zhou, S. W. Lin, A. Bian, Z. Q. Xiang, A. Iparraguirre, C. Lopez-Camacho, E. J. Wherry, H. C. J. Ertl, Adenoviral vectors persist in vivo and maintain activated $CD8^+$ T cells: Implications for their use as vaccines. *Blood* **110**, 1916–1923 (2007).
43. J. C. Ramírez, M. M. Gherardi, M. Esteban, Biology of attenuated modified vaccinia virus Ankara recombinant vector in mice: Virus fate and activation of B- and T-cell immune responses in comparison with the Western Reserve strain and advantages as a vaccine. *J. Virol.* **74**, 923–933 (2000).
44. R. S. Akondy, N. D. Monson, J. D. Miller, S. Edupuganti, D. Teuwen, H. Wu, F. Quyyumi, S. Garg, J. D. Altman, C. Del Rio, H. L. Keyserling, A. Ploss, C. M. Rice, W. A. Orenstein, M. J. Mulligan, R. Ahmed, The yellow fever virus vaccine induces a broad and polyfunctional human memory $CD8^+$ T cell response. *J. Immunol.* **183**, 7919–7930 (2009).
45. J. W. Northfield, C. P. Loo, J. D. Barbour, G. Spotts, F. M. Hecht, P. Klenerman, D. F. Nixon, J. Michaëlsson, Human immunodeficiency virus type 1 (HIV-1)-specific $CD8^+$ $T_{EMRA}$ cells in early infection are linked to control of HIV-1 viremia and predict the subsequent viral load set point. *J. Virol.* **81**, 5759–5765 (2007).
46. S. Sridhar, S. Begom, A. Bermingham, K. Hoschler, W. Adamson, W. Carman, T. Bean, W. Barclay, J. J. Deeks, A. Lalvani, Cellular immune correlates of protection against symptomatic pandemic influenza. *Nat. Med.* **19**, 1305–1312 (2013).
47. S. G. Hansen, J. C. Ford, M. S. Lewis, A. B. Ventura, C. M. Hughes, L. Coyne-Johnson, N. Whizin, K. Oswald, R. Shoemaker, T. Swanson, A. W. Legasse, M. J. Chiuchiolo, C. L. Parks, M. K. Axthelm, J. A. Nelson, M. A. Jarvis, M. Piatak, J. D. Lifson, L. J. Picker, Profound early control of highly pathogenic SIV by an effector memory T-cell vaccine. *Nature* **473**, 523–527 (2011).
48. A. Reyes-Sandoval, D. H. Wyllie, K. Bauza, A. Milicic, E. K. Forbes, C. S. Rollier, A. V. S. Hill, $CD8^+$ T effector memory cells protect against liver-stage malaria. *J. Immunol.* **187**, 1347–1357 (2011).
49. U. Karrer, S. Sierro, M. Wagner, A. Oxenius, H. Hengel, U. H. Koszinowski, R. E. Phillips, P. Klenerman, Memory inflation: Continuous accumulation of antiviral $CD8^+$ T cells over time. *J. Immunol.* **170**, 2022–2029 (2003).
50. J. Grebely, M. Prins, M. Hellard, A. L. Cox, W. O. Osburn, G. Lauer, K. Page, A. R. Lloyd, G. J. Dore; International Collaboration of Incident HIV and Hepatitis C in Injecting Cohorts (InC3), Hepatitis C virus clearance, reinfection, and persistence, with insights from studies of injecting drug users: Towards a vaccine. *Lancet Infect. Dis.* **12**, 408–414 (2012).
51. H. Price, R. Gilson, D. Mercey, A. Copas, J. Parry, A. Nardone, A. Johnson, G. Hart, Hepatitis C in men who have sex with men in London—A community survey. *HIV Med.* **14**, 578–580 (2013).
52. D. W. Porter, F. M. Thompson, T. K. Berthoud, C. L. Hutchings, L. Andrews, S. Biswas, I. Poulton, E. Prieur, S. Correa, R. Rowland, T. Lang, J. Williams, S. C. Gilbert, R. E. Sinden, S. Todryk, A. V. Hill, A human phase I/IIa malaria challenge trial of a polyprotein malaria vaccine. *Vaccine* **29**, 7514–7522 (2011).
53. S. H. Sheehy, C. J. A. Duncan, S. C. Elias, P. Choudhary, S. Biswas, F. D. Halstead, K. A. Collins, N. J. Edwards, A. D. Douglas, N. A. Anagnostou, K. J. Ewer, T. Havelock, T. Mahungu, C. M. Bliss, K. Miura, I. D. Poulton, P. J. Lillie, R. D. Antrobus, E. Berrie, S. Moyle, K. Gantlett, S. Colloca, R. Cortese, C. A. Long, R. E. Sinden, S. C. Gilbert, A. M. Lawrie, T. Doherty, S. N. Faust, A. Nicosia, A. V. S. Hill, S. J. Draper, ChAd63-MVA–vectored blood-stage malaria vaccines targeting MSP1 and AMA1: Assessment of efficacy against mosquito bite challenge in humans. *Mol. Ther.* **20**, 2355–2368 (2012).
54. M. Roederer, J. L. Nozzi, M. C. Nason, SPICE: Exploration and analysis of post-cytometric complex multivariate datasets. *Cytometry A* **79**, 167–174 (2011).
55. M. Toebes, M. Coccoris, A. Bins, B. Rodenko, R. Gomez, N. J. Nieuwkoop, W. van de Kasteele, G. F. Rimmelzwaan, J. B. Haanen, H. Ovaa, T. N. Schumacher, Design and use of conditional MHC class I ligands. *Nat. Med.* **12**, 246–251 (2006).
56. E. W. Newell, N. Sigal, N. Nair, B. A. Kidd, H. B. Greenberg, M. M. Davis, Combinatorial tetramer staining and mass cytometry analysis facilitate T-cell epitope mapping and characterization. *Nat. Biotechnol.* **31**, 623–629 (2013).


**Acknowledgments:** We would like to acknowledge BEI Resources for providing the HCV peptides and I. Poulton for support at the CCVTM Oxford. **Funding:** Supported by the Medical Research Council (MRC) UK and the European Union (Framework VI; HEPACIVAC) for funding the study and the manufacture of MVA-NSmut through an MRC UK DCS (Developmental Clinical Studies) award. E.B. is supported by the MRC as a Senior Clinical Fellow, the Oxford Martin Schools, and National Institute for Health Research Oxford Biomedical Research Centre. L. Swadling is

supported by an MRC CASE studentship. **Author contributions:** E.B., S. Capone, S. Colloca, J.H., A.F., R.C., C.K., A.N., and P.K. designed the study/protocols. L. Swadling, S. Capone., R.D.A., A.B., R. R., E.W.N., J.H., C.K., D.B., J.F., A.K., V.A., M.D.S., F.G., M.L.E., L. Siani, C.T., A.H., M.D., A.F., E.B., and P.K. performed the research and analysis. L. Swadling., E.B., A.F., S. Capone, and P.K. wrote the manuscript. E.B. was the principal investigator. **Competing interests:** S. Colloca, A.F., R.C., and A.N. are named inventors on patent applications covering HCV-vectored vaccines and chimpanzee adenovirus vectors [WO 2006133911 (A3) hepatitis C virus nucleic acid vaccine, WO 2005071093 (A3) chimpanzee adenovirus vaccine carriers, WO 03031588 (A2) hepatitis C virus vaccine]. P.K. has acted as a consultant to Tibotec and Pfizer on antiviral therapy. The other authors declare that they have no competing interests. **Data and materials availability:** The ChAd3-NSmut/MVA-NSmut vaccine study (HCV003) is registered in the ClinicalTrial.gov database (ID: NCT01296451).

Submitted 1 April 2014
Accepted 8 September 2014
Published 5 November 2014
10.1126/scitranslmed.3009185

**Citation:** L. Swadling, S. Capone, R. D. Antrobus, A. Brown, R. Richardson, E. W. Newell, J. Halliday, C. Kelly, D. Bowen, J. Fergusson, A. Kurioka, V. Ammendola, M. Del Sorbo, F. Grazioli, M. L. Esposito, L. Siani, C. Traboni, A. Hill, S. Colloca, M. Davis, A. Nicosia, R. Cortese, A. Folgori, P. Klenerman, E. Barnes, A human vaccine strategy based on chimpanzee adenoviral and MVA vectors that primes, boosts, and sustains functional HCV-specific T cell memory. *Sci. Transl. Med.* **6**, 261ra153 (2014).